INVESTIGATION OF CLOSE-SPACED THERMIONIC CONVERTER

TECHNICAL DOCUMENTARY REPORT ASD-TDR-62-687

October 1962

Directorate of Aeromechanics
Aeronautical Systems Division
Air Force Systems Command
Wright-Patterson Air Force Base, Ohio

Project No. 8173, Task No. 817305

(Prepared under Contract No. AF 33(616)-7683
by ITT Industrial Laboratories, A Division of International Telephone and
Telegraph Corp., Fort Wayne, Indiana; Donald K. Coles, author)

NOTICES

When Government drawings, specifications, or other data are used for any purpose other than in connection with a definitely related Government procurement operation, the United States Government thereby incurs no responsibility nor any obligation whatsoever; and the fact that the Government may have formulated, furnished, or in any way supplied the said drawings, specifications, or other data, is not to be regarded by implication or otherwise as in any manner licensing the holder or any other person or corporation, or conveying any rights or permission to manufacture, use, or sell any patented invention that may in any way be related thereto.

Items and materials used in the study, or called out in the report by trade name or specifically identified with a manufacturer, were not originated for use in this specific study or for applications necessary to this study. Therefore, the failure of any one of the items or materials to meet the requirements of the study is no reflection on the quality of a manufacturer's product or on the manufacturer. No criticism of any item or material is implied or intended, nor is any endorsement of any item or material by the USAF implied or intended.

Qualified requesters may obtain copies of this report from the Armed Services Technical Information Agency, (ASTIA), Arlington Hall Station, Arlington 12, Virginia.

This report has been released to the Office of Technical Services, U. S. Department of Commerce, Washington 25, D. C., in stock quantities for sale to the general public.

Copies of this report should not be returned to the Aeronautical Systems Division unless return is required by security considerations, contractual obligations, or notice on a specific document.

13-305M, 200, 12-13-62

Aeronautical Systems Division, Dir/Aeromechanics, Flight Accessories Lab, Wright-Patterson AFB, Ohio.
Rpt Nr ASD-TDR-62-687, INVESTIGATION OF CLOSE-SPACED THERMIONIC CONVERTER. Final report, Oct 62, 77 p. incl. illus., tables, 12 refs.

Unclassified Report

Difficulties in realizing a very small anode cathode spacing, due to uneven thermal expansion and warping, have led to a feasibility study of a subliming anode surface that automatically maintains the proper spacing from the cathode. Barium was chosen as a subliming metal since it serves also to activate the cathode. This required that all parts of the vacuum enclosure be held above 500°C. Effects of barium corrosion at high temperatures were studied. Four test models were made and tested. Starting with an anode-cathode spacing of 0.007 inch and a heated barium reservoir, the spacing was reduced by build-up of barium on the anode. The characteristic thermionic current-voltage curves were seen, with currents twelve times larger than those obtainable with the original spacing. The highest power output observed was 0.28 amperes/cm^2 at 0.7 volt. Since the temperature distribution in the anode was non-optimum, suggestions are made for further studies with improved anode design.

(over)

1. Generators
2. Thermionic Converters
3. Diodes
4. Servo mechanisms

I. AFSC Project 8173, Task 817305
II. AF33(616)-7683
III. ITT Industrial Laboratories, Fort Wayne, Indiana
IV. D. K. Coles
V. Aval fr OTS
VI. In ASTIA collection

Aeronautical Systems Division, Dir/Aeromechanics, Flight Accessories Lab, Wright-Patterson AFB, Ohio.
Rpt Nr ASD-TDR-62-687, INVESTIGATION OF CLOSE-SPACED THERMIONIC CONVERTER. Final report, Oct 62, 77 p. incl. illus., tables, 12 refs.

Unclassified Report

Difficulties in realizing a very small anode cathode spacing, due to uneven thermal expansion and warping, have led to a feasibility study of a subliming anode surface that automatically maintains the proper spacing from the cathode. Barium was chosen as a subliming metal since it serves also to activate the cathode. This required that all parts of the vacuum enclosure be held above 500°C. Effects of barium corrosion at high temperatures were studied. Four test models were made and tested. Starting with an anode-cathode spacing of 0.007 inch and a heated barium reservoir, the spacing was reduced by build-up of barium on the anode. The characteristic thermionic current-voltage curves were seen, with currents twelve times larger than those obtainable with the original spacing. The highest power output observed was 0.28 amperes/cm^2 at 0.7 volt. Since the temperature distribution in the anode was non-optimum, suggestions are made for further studies with improved anode design.

(over)

1. Generators
2. Thermionic Converters
3. Diodes
4. Servo mechanisms

I. AFSC Project 8173, Task 817305
II. AF33(616)-7683
III. ITT Industrial Laboratories, Fort Wayne, Indiana
IV. D. K. Coles
V. Aval fr OTS
VI. In ASTIA collection

FOREWORD

This report was prepared by the International Telephone and Telegraph Corporation on USAF Contract No. AF33(616)-7683. The contract was initiated under Project No. 8173, Task No. 817305. The work was administered under the direction of the Flight Accessories Laboratory, Aeronautical Systems Division, with Lt. O. P. Breaux and Mr. G. H. Miller acting as project engineers.

This is the final report on the contract, covering work conducted from December 15, 1960 to June 25, 1962. It was prepared by D. K. Coles under the supervision of Dr. R. T. Watson, Director of the ITT Industrial Laboratories in Fort Wayne, Indiana. The program was directed by D. K. Coles in close consultation with C. L. Day. Other ITT personnel actively associated with the project were E. Behun, F. Haak, H. Salinger and R. Weaver.

ABSTRACT

Difficulties in realizing a very small anode-cathode spacing, due to uneven thermal expansion and warping, have led to a feasibility study of a subliming anode surface that automatically maintains the proper spacing from the cathode. Barium was chosen as a subliming metal since it serves also to activate the cathode. This required that all parts of the vacuum enclosure be held above 500 degrees C. Effects of barium corrosion at high temperatures were studied. Four test models were made and tested, By holding the temperature of the barium reservoir constant and varying the cathode temperature, the maximum of the Taylor-Langmuir emission S-curve was repeatedly traversed. Starting with an anode-cathode spacing of 0.007 inch and a heated barium reservoir, the spacing was reduced by build-up of barium on the anode. A metallic connection between anode and cathode then developed. This was removed by raising the cathode above 1000 degrees C and the anode above 500 degrees C. The characteristic thermionic current-voltage curves were then seen again, but with currents 12 times larger than those obtainable with the original spacing. This proved that build-up of barium had reduced the anode-cathode spacing. The highest power output observed was 0.28 amperes/cm^2 at 0.7 volt. Since the temperature distribution in the anode was non-optimum, suggestions are made for further studies with improved anode design.

PUBLICATION REVIEW

The publication of this report does not constitute approval by the Air Force of the findings or conclusions contained herein. It is published for the exchange and stimulation of ideas.

TABLE OF CONTENTS

Section		Page
1.0	INTRODUCTION	1
2.0	THEORETICAL DISCUSSION - THE SUBLIMING METAL PRINCIPLE	2
2.1	Sublimation Control by Space Charge Limitation of Current Density	3
2.2	Effect of Close Spacing on the Anode Work Function	6
2.3	Sublimation Control by Very Close Approach to the Cathode	7
2.4	Efficiency of the Thermionic Converter	8
2.5	Temperature Distribution in the Cathode	13
2.6	Temperature Distribution in the Anode	13
2.7	Effect of Subliming Metal on Cathode Work Function	15
3.0	CONSTRUCTION OF TEST MODELS	16
3.1	Ceramic-to-Metal Seals	16
3.2	Machining and Welding of Tungsten and Tantalum	18
3.3	Testing of Materials with Hot Barium	18
3.4	Testing Electrical Insulation with Hot Barium	19
3.5	Filling, Final Pumping, and Sealing-Off	21
3.6	Low Temperature Diodes with Cadmium as Subliming Metal	21
4.0	EXPERIMENTAL TESTS OF MODEL CONVERTERS	22
4.1	Condensation and Sublimation of Barium at the Anode Surface	28
4.2	Activation of the Cathode By Sublimation of Barium	30
5.0	SUGGESTED IMPROVEMENTS IN TEST MODEL CONVERTER	31
6.0	SUMMARY AND CONCLUSION	31
BIBLIOGRAPHY		69
APPENDIX A	Summary of Test Results	70
APPENDIX B	Transient Solution for Internal Surface Temperature of Thermionic Converter Anode	71
APPENDIX C	Steady State Temperature Distribution Produced by a Source of Heat on One Surface of a Low Conductivity Slab with a Perfect Thermal Conductor on the Other Side	74
APPENDIX D	Collapsing Pressure of Thin Walled Cylindrical Vessels	77

LIST OF ILLUSTRATIONS

Figure		Page
1	Parallel Plane Thermionic Converter with Decoupling Layer of Low Thermal Conductivity Metal	33
2	Cylindrical Thermionic Converter with Decoupling Layer of Low Thermal Conductivity Metal	34
3	Thermionic Converter with Central Reservoir of Subliming Metal	35
4	Thermionic Converter with Peripheral Reservoir of Subliming Metal	36
5	Electron Energy Level Diagram for Thermionic Diode	37
6	Electronic Efficiency-Voltage Curves for Different Operating Temperatures	38
7	Thermionic Converter with Extended Anode for Radiation of Heat	39
8	Test Model of Subliming Metal Thermionic Converter	40
9	Cathode, Tantalum Envelope, and BeO Ceramic Insulator for Test Model	41
10	Anode for Test Model	42
11	Vacuum Brazing System	43
12	Tantalum Tube for Testing Materials with Hot Barium	44
13	Test of Brazing Alloy	45
14	Two-Electrode Cell for Materials Test	46
15	Two-Electrode Test Cell	47
16	System for Filling, Pumping, and Sealing-Off Test Models	48
17	Jig for Pinching-Off Tantalum Tubing	49
18	Low-Temperature Test Cell for Observations on Subliming Cadmium	50
19	Transparent Test Cell for Observations on Subliming Cadmium	51
20	High Voltage Electron Beam Equipment	52
21	Circuit for Testing Thermionic Converters	53
22	Side View of Thermionic Cell with Radiator, Showing Electron and Thermal Shields	54
23	Top View of Thermionic Cell with 6 Inch Diameter Radiator and Shields	55
24	Thermionic Cell with 12 Inch Diameter Radiator	56
25	Modified Equipment for Testing Thermionic Converter	57
26	Experimental Current - Voltage Curves	58
27	Experimental Current - Voltage Curves	59
28	Experimental Current - Voltage rves	60
29	Experimental Current - Voltage Curves	61
30	Experimental Current - Voltage Curves	62
31	Experimental Current - Voltage Curves	63
32	Experimental Current - Voltage Curves	64
33	Experimental Current - Voltage Curves	65

LIST OF ILLUSTRATIONS (Continued)

Figure		Page
34	Theoretical Current - Voltage Curves for Vacuum Thermionic Converter	66
35	R/J_s vs d for Nine Cathode Temperatures	67
36	Anode Design for Improved Localization of Barium Deposit	68
B-1	Temperature Rise of Thermionic Converter Anode Surface as a Function of Time	73
C-1	Steady State Temperature Distribution in Anode Decoupling Layer	75

LIST OF TABLES

Table No.		Page
1	Estimated Sublimation Pressure and Rate of Sublimation	5
2	Barium Corrosion	20
3	Barium Corrosion at 725 Degrees C	20
4	Data for Figures 26-29	26
5	Data for Figures 30-33	27

LIST OF SYMBOLS

a	anode
b	thickness of decoupling layer in cm
c	cathode
c	specific heat in joules cm^{-3} deg K^{-1}
d	anode-cathode spacing in cm
E	elastic modulus in lb in^{-2}
E_a	radiant emissivity of anode-to-space
E_{ca}	effective radiant emissivity cathode-to-anode
H_e	heat absorbed by the electron stream in watts
J_a	electronic current from the anode in amperes
J_c	electronic current from the cathode in amperes
K	thermal conductivity in watts cm^{-1} deg K^{-1}
p	mass density in gm cm^{-2}
P	pressure
q	heat flow in watts
Q	heat flux in watts cm^{-2}
S	sublimation rates (microns/min or cm/sec)
t	time interval in seconds, wall thickness in inches.
T	absolute temperature in degrees Kelvin
V	output voltage
V_a	anode potential in volts, measured between the Fermi level of the anode and the top of the electronic energy barrier
V_c	cathode potential in volts, measured between the Fermi level of the cathode and the top of the electronic energy barrier

w	anode-cathode spacing in cm
η	efficiency of thermionic converter
η_e	purely electronic efficiency
η_o	Carnot efficiency
ν	Poisson's ratio
ϕ_a	anode work function in volts
ϕ_c	cathode work function in volts

1.0 INTRODUCTION

It is generally recognized that development of a high efficiency vacuum thermionic generator has been seriously hindered by the presence of space charge in the gap between the hot cathode and the anode. This space charge is an obstacle which must be overcome before it is possible to construct really efficient thermionic generators. The obvious procedure of constructing diodes with extremely close spacing has proved to be difficult, due to expansion of materials, warping, disintegration, etc., over the operating life. Hence recent trends have been toward gas diodes in which the space charge is partially compensated by positively charged ions. These plasma diodes partially solve the space charge problem, but they introduce problems of their own which necessarily reduce their efficiency below that obtainable in principle from a vacuum diode with an extremely close spacing.

Therefore, in an attempt to make the high efficiency vacuum converter practical, ITT Industrial Laboratories in Fort Wayne has conducted a feasibility study for the Air Force on a novel method of obtaining and maintaining a very small anode-cathode spacing. This method automatically adjusts the spacing continuously by subliming a metal onto the anode surface. Local narrowing of the anode-cathode spacing allows an increased local current density, and this in turn raises the local temperature of the anode thus subliming away metal and closing the servo loop. The heat required to control sublimation of the anode is derived from the electron stream as it enters the anode and converts potential energy (corresponding to the anode work function) into heat.

In order to keep subliming metal on the anode, all other parts of the vacuum enclosure must be kept at the anode temperature or higher. This includes the electrical insulation between anode and cathode. Thus one of the requirements is a metal-to-insulator seal that will stand exposure to the subliming metal at a temperature somewhat above the anode temperature. In many cases a high anode temperature is desirable in order to either radiate away the waste heat or to supply a second stage of heat conversion which can make better use of a low heat rejection temperature.

There is still another reason for maintaining a high anode temperature - by so doing it may be possible to use the subliming metal to activate a tungsten cathode and thus obtain a high electron current density without seriously shortening the cathode life by evaporation of the tungsten. In nature, a copious emission of electrons from a single component material tends to be accompanied by rapid evaporation of that material. This problem can be solved by using a two component system such as a

---

Manuscript released by the author July 20, 1962 for publication as an ASD Technical Documentary Report.

tungsten cathode with a thin film of an electro-positive metal on its surface. Since the anode and the subliming metal reservoir must be the coolest locations inside the vacuum envelope, they will also be the main depositories for the electro-positive material used to activate the cathode. It therefore seems reasonable that the metal or mixture of metals supplied from the reservoir should serve the dual function of activating the cathode and regulating the narrow anode-cathode spacing.

Since barium is a favorite activator for cathodes, and has a fairly high sublimation pressure below its melting point, it was selected for initial experiments. Cesium or another activator may be included as a minor constituent in the vapor phase in order to lower the anode work function. It is believed that the effect of the low pressure of cesium on the cathode work function would be negligible and the concentration of cesium in the solid barium would be insufficient to lower the melting point of the barium appreciably. The cesium would reside mainly in the vapor phase and as a fraction of a monolayer on the surface of the barium. The anode temperature range in this case must be somewhere between 500 degrees C and the melting point of barium, which is approximately 800 degrees C. Other choices of spacing metal are possible; for example, manganese with a trace of cesium to lower the anode work function.

At very small anode-cathode spacings there is a possibility that low-level vibrations will produce a large modulation of the output current. There is also the possibility that close spacing will produce a significant reduction of the anode work function.

2.0 THEORETICAL DISCUSSION - THE SUBLIMING METAL PRINCIPLE

Because of the great difficulty in making and maintaining thermionic converters with an anode-cathode spacing as small as 0.0001 inch, ITT has proposed a servo mechanism for maintaining such a spacing. Starting with a spacing of several thousandths of an inch, a layer of subliming metal is allowed to build up continually on the anode surface. When the anode surface approaches close to the cathode, the spacing metal is heated locally and therefore resublimes, thus establishing kinetic equilibrium with a small spacing between anode and cathode. The local heating is brought about by local increase in the space-charge limited current from the cathode, by local reduction of the work functions, or even by contact with the immensely hotter cathode.

Diagrams of such converters are shown in Figures 1 and 2. The converter of Figure 1 has parallel plane cathode and anode surfaces. This construction is suitable for solar heating. The converter of Figure 2 has cylindrical cathode and anode surfaces, a construction which is suitable for heating in nuclear reactors. Both converters have a decoupling layer of metal of low thermal conductivity next to the inner anode surface. This may be an iron-nickel-cobalt alloy such as Ceramiseal or Fernico which have expansion coefficients matching that of pure alumina ceramic; or it may be the subliming spacer metal itself, such as barium. The use of a metal of low thermal conductivity allows a temperature rise of 20 or 30 degrees C to be developed by a reasonable current density of 5 or 10 amperes per square centimeter.

The subliming metal may be introduced originally into a separate reservoir held at a well defined temperature, as in Figure 3. In some cases, the reservoir may be removed after an initial curing period, as in Figure 4. In any case, the heat required to hold the reservoir at a fixed temperature will be very small if it is surrounded with laminar insulation consisting of thin metal foil separated by glass fibre with a high silica content.

4.1 Sublimation Control by Space Charge Limitation of Current Density

This section contains a quantitative discussion, including response time, for the special case where the effective work functions are independent of the anode-cathode spacing. We need equations for the temperature rise of the anode surface due to electron impingement, for the rate of change of the spacing as a function of temperature rise, and for the change of electron current as a function of the spacing.

The energy level for a vacuum thermionic converter is shown in Figure 5. The electronic heat absorbed from the cathode by the electron stream is[1]

$$(H_e)_c = J_c (V_c + 2kT_c/e) - J_a (V_c + 2kT_a/e) \quad (1)$$

Of this heat, the amount transformed into electrical power is

$$P_e = (J_c - J_a) (V_c - V_a) = J V \quad (2)$$

where $V = (V_c - V_a)$ is the output voltage. The electronic heat rejected at the anode is therefore, (by difference)

$$(H_e)_a = J_c (V_a + 2kT_c/e) - J_a(V_a + 2kT_a/e) \quad (3)$$

The main term J_cV_a may be thought of as the energy dissipated in the anode by the electrons "falling down" from the top of the space charge barrier in Figure 5 to the Fermi level in the anode. Let us assume for the moment that the anode emission current J_a is zero and that the voltage term in (3) is the order of 2 volts. Then if a slight local decrease of the anode-cathode spacing produces a local increase of current density ΔJ_c, the heating change on the anode surface, due to electrons converting potential energy into heat, will be

$$(\Delta H_e)_a = 2 \Delta J_c \text{ watts/cm}^2 \quad (4)$$

The first effect of this electronic heat transfer is to raise the temperature of the inner surface of the anode. To better control the temperature rise, the anode has a composite structure as indicated in Figure 1, consisting of a thin layer of metal of low thermal conductivity adjacent to the inner surface, with a thicker layer of metal with a high thermal conductivity bonded to it. The greater thermal conductivity of the thicker layer tends to "short-circuit" any temperature differences between different parts of the anode surface, so that for the moment we may assume its temperature

remains uniform and constant. While this assumption is not strictly true it allows us to focus attention on the shortest time constant. The effect of variable radiator temperature is additional regulation with a longer response time.

In the absence of subliming metal, a change of electron heating would eventually produce a local steady-state temperature rise at the anode surfaces equal to

$$\Delta T = \frac{b \Delta H_e}{K} = \frac{2b}{K} \Delta J_c \text{ deg C} \tag{5}$$

where K is the thermal conductivity, b is the thickness of the layer of low thermal conductivity.

A suddenly applied heat current will instantly start a temperature rise of the inner surface. However, before reaching its steady state value, the temperature rise will slow down and approach its asymptotic value exponentially with a time constant equal to $b^2 cp/K$. The approach to equilibrium is discussed in appendix B. For a layer of Ceramiseal 3 mm thick at 500 degrees C, the time required for a suddenly applied increase in heat current to produce a surface temperature rise to within 63 percent of its steady-state value is approximately 0.7 second. For the moment we may neglect this short delay and consider that the steady-state temperature rise is reached instantly.

If the rate of sublimation of spacing metal associated with a rise of temperature is dS/dT cm/sec, then the rate of change of the spacing "w" associated with a change of current will be

$$\frac{dw}{dt} = \frac{2b}{K} \frac{(dS)}{(dT)} \Delta J_c \text{ cm/sec} \tag{6}$$

The sublimation rates, S, for a number of different metals are shown in Table 1. These metals are mostly in column II of the periodic table and several are suitable for activating thermionic emission from a tungsten cathode. It should be noted that the data on sublimation pressures from different sources are often inconsistent so that the sublimation rates of Table 1 must be considered estimates. Much of the data in Table 1 were compiled by Dushman[2].

If we assume a barium sublimation rate of 6.5×10^{-5} cm/sec and a temperature derivative dS/dT equal to 2.6×10^{-6} cm/sec degrees K, together with the thermal conductivity K of Ceramiseal at 500 degrees C = 0.226 watt/cm degree C, and a thickness b = 0.3 cm, we find

$$\frac{dw}{dt} = 6.9 \times 10^{-6} \Delta J_c \text{ cm/sec} \tag{7}$$

Table 1

Estimated Sublimation Pressure and Rate of Sublimation

Pressure / Metal		10^{-5} mm	10^{-4} mm	10^{-3} mm	10^{-2} mm	10^{-1} mm	1 mm	T_{melt}
Cadmium	T[1]	148	180	220	264	321		321
	S[2]	0.021	0.20	1.9	18.5	180		
Zinc	T	211	248	292	343	405		419
	S	0.018	0.17	1.7	16	150		
Magnesium	T	287	331	383	443	515	605	651
	S	0.042	0.40	3.9	37	350		
Strontium	T	361	413	475	549	639	750	800
	S	0.050	0.48	4.6	44	420	4000	
Barium	T	418	476	546	629	730	858	800
	S	0.045	0.43	4.1	39	370	3500	
Calcium	T	408	463	528	605	700		810
	S	0.055	0.53	5.1	48			
Radium	T	300	350	410	480	570	670	960
	S							
Silver	T	767	848	963				961
	S	0.011	0.10	1.0				
Manganese	T	717	791	878	980	1103	1251	1260
	S	0.011	0.11	1.0	10	90	810	

1 T is the temperature in degrees C corresponding to the vapor pressures in the table

2 S is the speed of evaporation in microns per minute.

We must now find the magnitude of the spacing reduction that allowed the increase ΔJ_c in the space charge controlled current J_c. For calculating the effect of space charge on current, it is convenient to utilize a recent evaluation by Webster[3] of Langmuir's 1923 paper. If we assume a saturated current density of 20 amperes/cm^2 and a temperature of 1800 degrees K, and a spacing d = 0.000254 cm, then Webster's parameter R is equal to 18. Utilizing Webster's Figure 4 for this value of R and assuming that the value of V is slightly less than the contact potential, we find an approximate value for the ratio between change of spacing and change of current

$$\Delta w = 2.1 \times 10^{-5} \Delta J_c \text{ cm} \tag{8}$$

Comparing equations (7) and (8) we find

$$\frac{d(\Delta w)}{dt} = -0.33 \Delta w \tag{9}$$

Thus any departure from the equilibrium spacing will tend to be reduced. The spacing will approach its equilibrium value at an exponential rate. For the above parameters the time constant will be approximately 3 seconds.

If the barium atoms after sublimation were to travel in a straight line, the time required to leave a hot spot would be the order of 10^{-4} seconds. Even when we multiply this time by the number of independent starts made by the atom before leaving the vicinity due to collisions with anode and cathode (say 2000 starts) the atomic diffusion time is less than a second. Thus for sublimation pressure of 10^{-2} mm or lower, the rate of movement of barium is limited only by its sublimation rate.

2.2 Effect of Close Spacing on the Anode Work Function

If the pressure of the subliming metal is kept high, so that reduction of a local space charge barrier to zero still does not produce enough local current to stop the anode growth, then it is expected that the anode-cathode spacing will continue to decrease and may in some places become less than 0.0001 inch. This does not necessarily mean loss of stability, however, for in this case the current density may be increased by an effective reduction of the anode and cathode work functions. Since the exact value of the cathode work function is not important under these conditions, we may focus our attention on the all-important anode work function.

Observations with the field emission microscope[4] have revealed large local variations in work function. Thus the microscopic work function might vary from two to three volts over distances of the order of 10^{-5} inch, giving an average work function of 2.5. Over distances as small as 10^{-6} inch the microscopic work function might vary over a larger range -- say from one to four volts -- still giving an average work function of 2.5 volts. Close approach of the anode to the cathode makes it possible to utilize the lower range of work function. For example, consider an anode work function variable over its surface in accordance with the equation

$$\phi_a = W_o + W_1 \sin \frac{\pi x}{a} \tag{10}$$

Let the spacing be w and the cathode work function ϕ_c. Then the potential energy seen by an electron in the space relative to the Fermi level in the cathode, and measured at a distance z from the cathode is

$$\phi = \phi_c + \frac{z}{w}(V + W_o - \phi_c) + W_1 \sin\left(\pi \frac{x}{a}\right) \frac{\sinh\left(\pi \frac{z}{a}\right)}{\sinh\left(\pi \frac{w}{a}\right)} \tag{11}$$

If the quantity $V + W_o - W_1$ is greater than ϕ_c, then for large spacings the minimum barrier seen by the electrons is

$$\phi_{min} = V + W_o \qquad (z/a \gg 1) \tag{12}$$

while for very small spacings the minimum barrier seen by the electrons is

$$\phi_{min} = W + W_o - W_1 \qquad (z/a \ll 1) \tag{13}$$

Thus very small spacings will tend to increase the thermionic current and bring about further regulation of the anode-cathode spacing. At the same time the efficiency of operation should be increased.

It should be mentioned that in cells with large space charge barriers, or in which the cathode work function cannot be sufficiently reduced, the magnitude of the cathode work function is indeed of prime importance and is often greater than $V + \phi_a$. Actually, in many devices it may be desirable to make $V + W_o + W_1$ slightly less than ϕ_c. Electron emission from tungsten has recently been the subject of interesting studies by Coomes[5].

2.3 Sublimation Control by Very Close Approach to the Cathode

If the pressure of subliming metal from the reservoir is sufficiently high, it will continue to deposit on the anode surface even at the highest currents which can be drawn from the cathode. Then, as the anode surface gets closer to the cathode, the heating produced by the electron current will level off, since space charge no longer inhibits it. The heating by radiation and by gaseous conduction tend to be independent of the spacing when the spacing is small. As the two surfaces approach each other the time of flight of the heat-carrying atoms is reduced - but so also is the number of atoms in the intervening space (at constant pressure), thus the two effects tend to cancel.

Later, as the anode surface approaches within one millionth of an inch of the cathode, the rate of diffusion of metal atoms to the point of closest approach is greatly slowed, due to the innumerable collisions which each atom must make on its way to this point. Finally there is simply no more room for spacer atoms on the anode surface without touching the cathode. At this point the growth of the layer of spacer metal is stopped. The much higher temperature of the cathode discourages a build-up of spacer metal in thermal contact with the cathode. Experience has shown that when the anode surface is cool, a short circuit may occur, which will disappear when the anode is heated to 500 degrees C.

It is true that barium atoms adhere more tenaciously to a clean tungsten surface than to solid barium metal, but this strong pull of tungsten or tantalum extends only to a first monolayer of barium atoms. At the operating cathode temperature, the adhesion is strong enough to keep only a fraction of a monolayer on the cathode surface. Barium atoms, attempting to lodge between the anode and cathode surfaces, are driven off by the high temperature of the cathode. Even barium atoms already entrenched on the cathode surface tend to drive off newcomer barium atoms.

The close approach of the two surfaces tends to reduce the vapor pressure from the "combination" of the two surfaces. On the other hand, the work function of each surface for thermionic emission to the other tends to be reduced. Thus one may expect to find here an exception to the general rule that low work function is accompanied by high vapor pressure[6]. A reduction of work function for both anode and cathode would in principle make possible a thermionic converter of very high efficiency. There are two separate but related advantages:

a. The energy lost by radiation can be reduced below that carried by the electrons.

b. The energy wasted by the electrons "falling down" the anode work function can be reduced, while the effective cathode work function V_c can be maintained at a much higher value. Thus the output voltage could be large. This point is discussed in the following section.

Vibrations and effects due to temperature changes are expected to confuse the picture. In our experiments these effects were minimized by making the cell spacer relatively rigid. This less predictable aspect of the subliming metal principle can be studied at lower temperatures, since a high current density is not essential for its investigation. An experimental cell to study the sublimation of cadmium at a relatively low temperature is described in Section 3.6.

2.4 Efficiency of the Thermionic Converter

Numerous discussions of converter efficiency have been published[1,3,6-9]. This section contains remarks pertinent to the subliming metal converter together

with a general discussion of converter efficiency. Efficiency of a heat-to-electrical-power transducer is defined as the ratio of output power to input heat. It may be remarked that efficiency is only one of several figures of merit for the transducer. For example the source of cold might be more expensive than the source of heat, in which case a more important figure of merit would be the ratio of output power to input cold.

Several factors which reduce efficiency may be separated out and enumerated.

a. The Carnot efficiency $1 - T_a/T_c$ is always less than unity in practice. In space applications where unused heat must be radiated away and weight is important, the ratio T_a/T_c may be necessarily greater than one half.

b. The anode work function may be higher than is necessary to prevent electron emission from the anode at the chosen anode temperature. This reduces the electric power and generates waste heat in the anode.

c. In operation, a space charge potential minimum usually exists in the space between anode and cathode. This has the same effect as b. in reducing the output power and generating waste heat in the anode. With a "patchy" anode, the current-average of the anode work function is reduced when the anode-cathode spacing is reduced.

d. The use of space charge to control heating of the anode surface implies that the cathode emission current is never fully used. This is not an inefficiency in itself, since electrons returned to the cathode extract no net heat from it: it represents a loss only in that it reduces the ratio of the energy carried by electrons to the energy carried by radiation and thermal conduction. In conventional vacuum thermionic diodes, space charge usually restricts the power output seriously.

e. The electrical lead loss to the cathode is comparatively low and in some cases can be largely eliminated by making good electrical connection to the low temperature end of the vacuum envelope.

f. In converters employing a neutral gas there is electrical power loss by electron collisions with the gas atoms and heat loss by thermal conduction through this gas. These losses tend to be proportional to the gas pressure. For a given pressure, the electrical loss increases with the spacing and the thermal loss decreases.

g. In converters employing an ionized gas there are the same losses as f. plus the heat or power expended in ionizing the gas.

h. In a subliming metal converter a temperature drop in the anode may be introduced in order to control sublimation of the spacer metal. It is

estimated that a temperature drop ranging up to 20 degrees C should be adequate for controlling sublimation of the spacer metal when the heat source is electron impingement on the anode. This may be considered either a utilization of the above mentioned waste heat b. or a slight restriction on Carnot efficiency a. depending on circumstances.

i. Heat conducted from the cathode through the vacuum envelope tends to be proportionately low for large concentrated converters, if minimum envelope thickness is limited by corrosion and leakage.

j. Temperature drop in thermal conduction from the inner anode surface to the final heat sink tends to be proportionately high for large concentrated converters.

k. Heat lost as radiation from the cathode tends to be proportional to the fourth power of the temperature. The effective cathode-to-anode emissivity should be kept low and any uninsulated area exposed to the sun should be kept low compared to the thermionically emitting area.

l. In case space charge control is not utilized and the spacer metal is allowed to build up until it comes almost into contact with the cathode, then in the act of limiting further deposition of atoms on the anode some heat will in all probability be transferred from the cathode to the anode. The amount of this heat transfer has not been estimated since it is likely to depend on such parameters as vibration level and irregular temperature fluctuations. In the ideal vibrationless constant temperature condition it appears that this heat transfer would be negligible because of the slow rate at which subliming metal atoms can transfer into the very narrow anode-cathode space.

It is convenient to express the efficiency as a product of a purely electronic efficiency, η_e, and a modifying factor, F, which is less than unity

$$\eta = \eta_e \cdot F \tag{14}$$

It is shown in the following paragraphs that by varying the output voltage it is possible in principle to achieve an electronic efficiency which closely approximates the Carnot efficiency. However, with present materials it is impossible to obtain a high value of the Carnot efficiency and of F at the same time.

If the current in a thermionic diode is considered to be the difference of two electron currents J_c and J_a originating in the cathode and anode respectively, not interacting with each other except through their over-all space charge, then the net current to the bus bar can be written $J = J_c - J_a$. Referring to Figure 5, the energy required to lift an electron from the Fermi level of the cathode to the top of the space charge hump is V_c electron-volts and the corresponding energy from the anode is V_a

electron volts. Neglecting the voltage drop in the leads, the voltage at the bus bar is $V = V_c - V_a$. The output power is then

$$P_e = (J_c - J_a)(V_c - V_a) \tag{15}$$

The heat conducted from the cathode by the electrons is

$$(H_e)_c = J_c (V_c + 2kT_c/e) - J_a (V_c + 2kT_a/e) \tag{16}$$

The heat which is dissipated in the anode is the difference of (15) and (16)

$$(H_e)_a = J_c (V_a + 2kT_c/e) - J_a (V_a + 2kT_a/e) \tag{17}$$

The purely electron efficiency is therefore

$$\eta_e = \frac{(J_c - J_a)(V_c - V_a)}{J_c (V_c + 2kT_c/e) - J_a (V_c + 2kT_a/e)} \tag{18}$$

The currents may be calculated from the equations

$$\begin{aligned} J_c &= A\, T_c^2 \exp(-V_c/kT) \\ J_a &= A\, T_a^2 \exp(-V_a/kT) \end{aligned} \tag{19}$$

Equation (18) then takes the form

$$\eta_e = \frac{v}{1 + 2b + \dfrac{2b\eta_o(1-\eta_o)^2}{\exp\left[b\left(\dfrac{1-\eta_o-v}{1-\eta_o}\right)\right] - (1-\eta_o)^2}} \tag{20}$$

where

$v = V_c - V_a/V_c$ = relative output voltage

$b = kT_c/V_c$ = relative cathode temperature

$\eta_o = T_c - T_a/T_c$ = temperature factor.

The electronic efficiency is plotted in Figure 6 as a function of the relative output voltage, for nine different values of the temperature factor. The curves for different values of the temperature have a common asymptote, whose equation is

$$\eta_e = \frac{v}{1 + 2b} \tag{21}$$

This equation may be derived from equation (20) by inserting the value $\eta_e = 1$, corresponding to zero thermionic emission fromthe anode. For all other values of η_e, the electronic efficiency reaches a maximum near $v = \eta_o$, at which point the cathode current falls below the anode emission and the efficiency drops rapidly to zero.

The small circles corresponding to the points $\eta_e = v = \eta_o$, lie on a line corresponding to the Carnot efficiency. It is seen that the peak electronic efficiency for each value of η_o nearly attains the Carnot value. While the curves shown are for the special value b = 0.05, curves for other values of b would appear very similar.

The modifying factor, F, of equation (14) may now be considered briefly. In the vacuum converter, (neglecting voltage drop in the lead wire), it is roughly approximated by

$$F = \frac{H_e}{H_e + H_o} \tag{22}$$

where H_e is the heat transported from the cathode by the electrons and H_o is the heat transported from the cathode by other means.

Our main aim must then be to attain a ratio H_e/H_o well above unity. It is of course true that the breakdown of equation (14) is by no means into independent factors, for the process of increasing $V_c - V_a$ in equation (18) to its optimum value would be accompanied by an exponential decrease of the ratio H_e/H_o.

In most vacuum converters that have been built, the effective work function V_a, considered as an independent variable, is too large for good efficiency unless the absorbtivity for radiation can be made considerably less than the absorbtivity for electrons. In the subliming metal converter, the value of V_a can be reduced toward its minimum value ϕ_a by reduction of the space charge barrier. There are then two possibilities for reducing ϕ_a below the natural work function of the spacing metal (say magnesium, barium, silver, or manganese).

a. Cesium and/or other impurities may be included as a minor constituent in the vapor phase in order to produce a fraction of a monolayer on the surface and thereby reduce its work function. According to Nernst' s distribution law[10] the concentration of cesium should be less in the spacer metal than in the vapor phase because the spacer metal has a lower vapor pressure than cesium. Thus the concentration of cesium in the spacer metal should have little effect on its melting point.

b. When the anode surface is allowed to come into close proximity with the cathode, a stable condition may be set up as described in the preceding section whereby the work function for transfer of electrons between cathode and anode is materially reduced.

2.5 Temperature Distribution in the Cathode

At practical cathode temperatures the thermionic emission is strongly sensitive to the local temperature but the radiation loss varies as only the fourth power of the temperature; thus the operating efficiency of the converter is rather sensitive to small variations in temperature over the cathode surface. Cool parts of the cathode lower the over-all efficiency. Ordinarily, hot spots on the cathode will tend to evaporate away any thermionically active emissive film on the cathode surface, or perhaps part of the cathode structure itself, thus shortening its useful life. For a cathode temperature of 1500 degrees K, a 1 percent change in T produces almost 20 percent change in current density. Thus different parts of the emitting surface should preferably be maintained at the same temperature within 15 degrees K.

2.6 Temperature Distribution in the Anode

The problems of temperature distribution in the anode are somewhat the same as those with the cathode; the temperature drop due to the irreversible flow of heat from the inner surface to the final heat sink should be kept low in most cases, and the range of temperature over the inner surface of the anode on open circuit should be kept small. When the electrical circuit is closed, the temperature will tend to equalize over the inner surface of the anode, and previously present small temperature differences will be translated into differences in current density.

$$\Delta J_c = \frac{K}{b V_a} \cdot \Delta T \tag{23}$$

For a decoupling layer of Ceramiseal 3 mm thick at 500 degrees C backed by a perfect thermal conductor, this turns out to be 0.4 amperes per degree C. Thus for a current density of 10 or 15 amperes/cm^2 the temperature of the anode surface on open circuit should preferably be held uniform within 8 degrees C. Larger variations in open-circuit temperature will lead to some loss of efficiency at the hot spots, brought about by sublimation of the spacing metal and space charge reduction of the current. Higher current densities will alleviate this difficulty by producing larger servo temperature rises.

The total servo temperature rise produced by a current density of 10 amps/cm^2 is the order of 27 degrees C. In badly designed cells with large temperature differences on open circuit, which exceed the servo temperature drop produced on closed circuit, it will be impossible to maintain a space charge limited current density over the whole surface of the anode. Two choices are then possible.

a. The excessively hot parts of the anode can be operated at zero current density, thus reducing the efficiency.

b. The pressure of subliming metal can be raised to reduce the space charge gap at the hot spots and allow spacing metal to built up on the cold spots until it approaches within a millionth of an inch of the cathode. The metal bridge can be prevented from making actual contact with the cathode because of the much greater heat of the cathode, which instantly vaporizes the spacing metal in the immediate vicinity of the contact.

In order to obtain automatic regulation of the spacing, we desire a test cell with a large area of the anode at constant temperature. The construction shown in Figure 1 lends itself well to this purpose, since the thick copper substrate tends to short-circuit external thermal currents and thus prevents them from adversely affecting the temperature on the inner surface. It also tends to localize heating effects produced by the local irregularities in the anode-cathode spacing, and thus correct them point by point. The temperature distribution produced by a point source of heat on the inner surface is given in Appendix C, equation (2). The rise of temperature is largely confined to a circle of radius equal to the thickness, b, of the layer of low thermal conductivity metal, and outside this circle falls off as the inverse cube of the distance.

A considerable amount of heat flows from the cathode to the anode via the external envelope, which may be of tantalum or zirconium. This is shown in Figure 7. Taking a thermal conductivity for tantalum of 0.45 watt/cm deg C, a thickness of 0.01 cm = 0.004 inch, and a conducting length of 0.3 cm, we find a thermal conductance of 0.015 watts/cm degree C. If the cathode temperature is 1500 degrees K and the anode temperature is 900 degrees K, the heat flow around the circumference will be 9 watts/cm. This heat flow serves a useful purpose in raising the temperature of the ceramic (about 70 degrees C if the anode is slotted as in Figure 7) thereby preventing condensation of spacer metal on the interior surface of the ceramic, but it tends to destroy the uniformity of temperature of the rest of the interior anode surface. The calculations in Appendix C show that for a thin layer of low conductivity metal backed by a perfect conductor the temperature rise is mostly confined to the immediate neighborhood of the tantalum envelope, and that away from this neighborhood the temperature rise falls off as the inverse square of the distance.

Appendix D discusses the possibility of atmospheric pressure buckling the thin tantalum envelope. It shows that for a 1-1/2 inch diameter cell and a wall thickness of 0.004 inch, the factor of safety is 20.

In some cases the large heat leak in the envelope may be eliminated as with the construction of Figure 2, or in a parallel plane geometry with solar heating through a sapphire window. However, the ceramic must be kept hot to prevent condensation of the spacing metal on it. This may be accomplished by judiciously placed slots as in Figure 1, or external radiative shields as in Figure 2. The temperature distribution produced by a slot was calculated and was also explored experimentally by means of an analogue field plotter. Radiation barriers may

consist of single sheets of metal or of multiple sheets of metal foil separated by glass fibre with a high silica content.

In space applications the heat reaching the anode must be radiated away. If the heat is simply radiated from the back of the anode, so that the radiating area is approximately equal to the internal surface area exposed to the cathode, then the anode temperature will approach the value

$$T_a = T_c \left[\frac{E_{ca}}{E_{ca} + E_a} \right]^{1/4} \tag{24}$$

where

E_{ca} is the effective radiant emissivity of cathode to anode

E_a is the radiant emissivity of anode to space

If this temperature is high enough to produce a large back electron emission from the anode, then in small converters the anode area can be increased as shown in Figure 7. Large power converters could be made up of many such converters well spaced from each other. In the case of large concentrated power converters such extensions would have an increased weight per watt of power, and the temperature drop in the copper may become so large as to be prohibitive. Thus large power converters in space should either radiate the heat right off the back of the anode surface exposed to the cathode, or else be provided with liquid cooling.

2.7 Effect of Subliming Metal on Cathode Work Function

Unless a tungsten cathode is provided with a film of electropositive material to reduce its work function, its temperature for good efficiency must be so high that its life will be seriously limited by evaporation. Becker[11] found that when barium atoms were absorbed on a tungsten surface the work function was reduced to as low as 2.1 volts, depending on the fraction of a monolayer present. Others have found still lower values. As discussed in Section 2.4, a higher electron barrier than this may be desired for optimum efficiency. In this case, it may be obtained by simply raising the back voltage on the anode, provided the resulting tendency for a deep space-charge potential minimum is eliminated by a sufficiently small anode-cathode spacing.

A favorite type of cathode in the electron tube industry is the dispenser cathode, in which a surface film of barium is continuously replenished at the operating temperature by flow of the barium through a porous substrate. Unfortunately, at the temperatures necessary for high efficiencies, the reservoir tends to be depleted in a relatively short time.

A second method of maintaining the active film on the tungsten surface is to re-evaporate or sublime it back to the tungsten surface continually. This method has already been used successfully with cesium plasma converters. The use of barium instead of cesium is an advantage in our application, however, because available evidence indicates that barium atoms remain attached to the tungsten surface, particularly the 211 crystal plane, at higher temperature than do cesium atoms. Furthermore, because it is not necessary to provide positive ions in the very close spacing of our cell, the cathode work functions need not be kept high but can be lowered without regard to the necessity of producing positive ions. The pressure of barium vapor required to produce a given fraction of a monolayer on tungsten at a given cathode temperature appears to be less than the corresponding pressure for cesium.

Mueller found by the method of field emission spectroscopy that small groups of atoms were strongly bound at 1500 degrees K even with no re-evaporation back to the tungsten.

If the anode is allowed to approach within 10^{-7} cm of the cathode, the work function of both cathode and anode will be reduced. If a stable condition can be set up with this small spacing, it may be possible to use a less electropositive spacer metal than barium, such as magnesium or manganese.

3.0 CONSTRUCTION OF TEST MODELS

Six vacuum-tight test models were constructed. Four of these were filled with barium. A photograph of a test model containing barium is shown in Figure 8. The cathode, tantalum envelope, and ceramic insulator, are sketched in Figure 9. The anode is sketched in Figure 10. Before assembly, a 3/16-inch diameter tantalum tubulation is brazed into the top part of the anode, and the tantalum envelope is welded to the top part of the tungsten or tantalum cathode. Then the anode assembly, ceramic insulating ring, and cathode assembly are brazed together in one operation.

3.1 Ceramic-to-Metal Seals

High alumina and beryllia ceramics rings are used to insulate the anode from the cathode. Ceramics used have been approximately 96 percent alumina, which softens at 1650 degrees C, approximately 99.5 percent alumina, which is semi-transparent, with a maximum working temperature of 1725 degrees C, pure alumina, with a melting point of 2040 degrees C, single crystal sapphire, and beryllium oxide. Boron nitride ceramics were tested for compatibility with hot barium but no seals were made with these ceramics. Rings were cut to size by ITT with a Cavitron ultrasonic cutting machine.

The usual method used for sealing the ceramic ring to the tantalum envelope and to the decoupling disc is by brazing. Brazing techniques have been described by Kohl[12].

Prior to brazing, the ceramic is coated with a molybdenum metallizing coat. This is brushed on while in a lathe and fired in wet hydrogen at temperatures up to 1525 degrees C, for times usually less than 1 hour. The composition of two metallizing mixtures used are given below.

Metallizing Mixture No. 1

160 g molybdenum powder (200 mesh)
40 g manganese powder (150 mesh)
100 ml nitrocellulose
50 ml amyl acetate
50 ml acetone

Metallizing Mixture No. 2

175 g molybdenum powder (200 mesh)
44 g manganese (200 mesh)
9 g titanium hydride
45 ml nitrocellulose lacquer
25 ml methyl ethyl ketone
50 ml ethyl ether
55 ml acetone

Before each metallizing operation these mixtures were ball milled for 24 hours. Metallizing mixture No. 2 could be fired at a lower temperature, but mixture No. 1 was preferred because it is believed that it will stand up better to barium at high temperatures. It is difficult to wet these metallizing coats with most brazing compounds, so that it is customary to apply a nickel coat to them to improve the wetting action. In most cases, nickel was electroplated on to a thickness of approximately 0.0001 inch in a nickel-chloride bath. Thicker coats tended to blister on firing. This coat was fired in wet hydrogen at 1000 degrees C for 10 minutes.

Since nickel tends to be attacked by barium, platinum was used instead in some cases. The platinum coat was not so easily wet as nickel, but some vacuum tight brazes were obtained with it. Figure 11 shows a 3/4 inch diameter seal.

Since tantalum reacts with hydrogen, all brazing was carried out in a vacuum. Some brazing was done in a 4-inch diameter vacuum furnace, but a preferred method was to heat the parts to be brazed by induction heating in a bell jar vacuum system. Figure 11 shows a photograph of this system. The cylindrical weight shown is used to hold the parts together while brazing. The parts to be brazed are mostly heated by radiation from a group of graphite coupling rings. The bell jar method has the great advantage that the moment of melting and of wetting the joint can be determined visually.

The brazing alloys used were nickel-gold and palladium-cobalt. The first of these has a liquidus temperature of 950 degrees C. The second has a liquidus temperature of 1235 degrees C. Copper-gold was also tried, but this appeared unable to resist barium at elevated temperatures.

Seals to the thin tantalum envelope were usually found to be vacuum tight. Seals could also be made between the flat side of the ring and thin sheets (0.010 inch) of tantalum, but thick blocks of tantalum cracked the ceramic. When attempts were made to braze Ceramiseal with the palladium alloy, the Ceramiseal tended to melt. Vacuum-tight seals to heavy blocks of Ceramiseal were easily made with the nickel-gold brazing alloy. All seals were checked for vacuum tightness with a helium leak tester.

Following the development of satisfactory brazing techniques, the metallizing furnace was modified to take larger cells. Thereafter it proved impossible to get satisfactory metallizing, probably due to the temperature being too low and uncontrollable. It was then necessary to purchase rings which had already been metallized.

3.2 Machining and Welding of Tungsten and Tantalum

Tungsten and tantalum were fabricated according to instructions supplied by the Fansteel Metallurgical Corporation. The tungsten cathode was ground into shape using a soft grinding wheel, dressed with a diamond.

The tungsten or tantalum cathode is welded to the tantalum envelope with an electric welding torch in an argon atmosphere. The welding box is gas tight, with an entry for argon at the bottom and exit at the top. Argon must be allowed to flow for at least one half hour at a rate of at least 10 cubic feet per hour before attempting to weld. Higher flows and longer flow times appear to give less oxidation at the weld. All welds were checked with a helium leak tester.

Better control was assured by mounting the parts to be welded on a rotating table, driven by a geared-down variable speed motor. Satisfactory welds have been made with both tungsten and tantalum cathodes. In the final cells the wall thickness was reduced to 0.004 inch by machining away tantalum after the weld was made, to reduce heat conductance.

3.3 Testing of Materials with Hot Barium

Materials were tested by sealing a weighed sample of the material together with barium in a tantalum tube, and heating in a vacuum furnace, usually at 725 degrees C for a period from 1 to 10 days. One of the tubes is shown in Figure 12. The tube is then broken open in a box filled with argon and the contents examined through the glass cover with the aid of an eyepiece. The samples are then removed from the inert atmosphere and examined more minutely with the aid of a microscope.

During this period, the barium oxidizes. Samples are then dropped into water to remove excess barium, and re-examined with the microscope. Unbroken samples are reweighed and the gain or loss of weight noted.

The samples may be in contact with solid barium, or only with barium vapor. In the latter case the tube is indented to keep the sample at the opposite end of the tube from the barium, and the sample is placed at a slightly hotter part of the furnace (as determined with a thermocouple) to minimize condensation of barium vapor on the sample. The tube is surrounded by an inert atmosphere during outgassing. The barium used in these tests was supplied in a long iron tube about one eighth inch in diameter. A piece of iron tube was freshly broken off at each end before it was inserted in the tube and the pump started.

Results of this investigation are qualitative at the present time. The barium may attack a sample in an apparently erratic manner, making a deep groove in one place and leaving the rest of the surface intact. Some tests were obviously run too long - no trace of the sample was found. Other tests were not run long enough to show any effect. The degree of vacuum is the earlier tests is questionable; the vacuum was improved in later tests. Some results of the weight measurements are shown in Table 2. Qualitative results on some other pure metals and brazing alloys are shown in Table 3.

The ceramics tested were 96 percent Al_2O_3, 99.5 percent Al_2O_3, and pure Al_2O_3, boron nitride and beryllium oxide. The 96 percent Al_2O_3 was attacked slightly when in contact with barium metal for a week at 750 degrees C. The 99.5 percent Al_2O_3, pure Al_2O_3, and beryllium oxide were not seriously damaged. The boron nitride appeared to react slightly. The sapphire was attacked, probably because it was not pure.

Copper and nickel showed a tendency to alloy with barium. Ceramiseal picked up a little weight. Tests were run with gold, platinum, nickel-gold, and the metallizing coats, but these results were not conclusive. Barium attacked silica and calcium aluminosilicate glass strongly. Figure 13 shows a cell with a nickel-gold braze before and after exposure to barium for 60 hours at 125 degrees C.

3.4 Testing Electrical Insulation with Hot Barium

The ceramic insulator in a thermionic converter must maintain its insulating property while exposed to hot barium vapor. During the course of testing ceramic samples heated with barium in a tantalum tube, such samples after exposure were tested for electrical conductivity along their surface. Although those tests were negative, they were not conclusive proof that a conducting surface did not form in the vacuum and then lose its conductivity when exposed to air. Therefore two-electrode cells were made and barium sealed into them. They were heated for several days in a vacuum furnace and the resistance between the electrodes measured without opening the cell. These tests also provided further information regarding

Table 2

Barium Corrosion

Material	Time (hours)	Weight Change (mg/cm^2)	Temp.	State (Solid-Vapor)
BeO	360	+ 0.55	725	V
Ceramiseal	138	+ 0.1	725	V
Ceramiseal	360	-2.7	725	S
Titanium	138	+ 0.1	725	V
Titanium	360	-1.4	725	S
Sapphire	360	-35	725	V
99.5% Al_2O_3	183	12.5	740	V
99.5% Al_2O_3	183	26.5	740	S
Pure Al_2O_3	183	10.8	740	S

Table 3

Barium Corrosion at 725 ^{o}C

Material	Condition
Iron	good
Zirconium	good
Tantalum	good
Platinum	poor
Palladium	poor
Nickel	poor
Copper	poor
Gold	poor
Palladium-cobalt	good
Nickel-gold	fair
Copper-gold	poor

the reliability of the ceramic-to-metal seal when exposed to hot barium. Cells of this type are shown in Figures 14 and 15.

It appeared that the ceramics retained their insulating property provided that the ceramic was held 10 degrees C above the temperature of the barium reservoir, and provided a leak did not develop. Some leaks developed that were attributed to brittleness of the tantalum from outgassing by heating in air. Thereafter the cells were pumped during outgassing with an argon atmosphere surrounding the tantalum tube.

3.5 Filling, Final Pumping, and Sealing-Off

In ordinary cells, oxygen-free copper tubing is used for the tubulation, and pinching-off presents no great difficulty. Our first tests with copper indicated that it alloys with barium and cannot be used. We have found that well annealed tantalum tubing can be pinched-off and that the resulting seal will stand many days of exposure to barium at 750 degrees C, with frequent temperature cycling. The tubing was 1/4-inch or 3/16-inch diameter with 0.015 wall.

Barium was purchased in hermetically sealed cans. In order to prevent oxidation of the barium, the can and the cell were placed in a sealed box filled with argon. After opening the can, a weighed amount of barium was inserted into the tubulation and the cell and the end of the tubulation attached to an assembly such as that shown in Figure 16, which has been previously flushed with argon. The cell was attached to a diffusion pump and outgassed by heating in an inert atmosphere. The cell was then separated from the pump by a copper pinch-off. Further pumping was done with a portable ion pump, which also could be used to measure the pressure. Finally the thermionic converter was sealed off at its tantalum tubulation.

A photograph of the pinching-off jig is shown in Figure 17. The tubulation is inserted between two lengths of hardened drill rod or between one length of drill rod and a length of flat tool steel; then a pressure of 5 to 10 tons is applied from above, forcing the upper drill rod down and pinching the tubulation. After this cold-welding operating the tubulation may not be completely severed, in which case it is flexed a few times until it breaks at the thinnest part. The pinched-off tube almost invariably tests vacuum tight with a helium leak detector. It was found that the sharp edge of the pinched-off tube could be lightly heliarced while the tube was on leak test, without any sign of leak showing up during this arc-welding.

3.6 Low Temperature Diodes with Cadmium as Subliming Metal

The construction of a high temperature cell is necessary to test the principle of sublimation control by space charge limitation of current density, as discussed in Section 2.1. A low temperature cell is believed adequate for testing the principle of sublimation control by very close approach to the cathode, as discussed in Section 2.3, and for studying current-voltage curves at very low anode-cathode spacings.

The subliming metal in this case can be cadmium, which develops a sublimation pressure of 10^{-3} mm at 220 degrees C. At this low temperature, cell construction is much easier, and it proved practical to construct cells with Kovar electrodes and an envelope of 7052 glass. Such a cell has the great advantage that movement of the spacer metal can be monitored visually. A photograph of one of these cells is shown in Figure 18. Sublimation of cadmium could be observed in these cells without damaging the glass, provided the cells were not overheated. Attempts were also made to construct a higher temperature transparent cell using calcium aluminosilicate glass and molybdenum electrodes. A sketch of this cell is shown in Figure 19. The molybdenum matches the thermal expansion of this glass, but in order to be sealed to the glass, the molybdenum was coated with a film of chromium. This was then oxidized before sealing to the glass.

The first cell was sealed in air, so the chromium oxide was left intact to protect the molybdenum against oxidation. It then proved impossible to remove the insulating film of chromium oxide on the inaccessible surfaces of the electrodes. Cell No. 2 was glassed in air, then the interior oxide surfaces removed by vapor blasting. Final assembly of the two electrodes inside the 1723 glass envelope was by means of high temperature glass frit at 750 degrees C in a vacuum furnace. The cell leaked. Experiments with transparent cells containing cadmium were discontinued in September 1961, following a review meeting with Mr. G. H. Miller, R. A. Garrett and Captain E. F. Redden at the Flight Accessories Laboratory. Since construction of the test models containing barium was proving more difficult than expected, it was decided that full effort should be expended on the cells containing barium.

4.0 EXPERIMENTAL TESTS OF MODEL CONVERTERS

The cell testing program aims were to reach an understanding of conditions inside the thermionic cell, with particular reference to the effective anode-cathode spacing and the movement of spacer metal. Since the thermionic converter is intended for a power supply in a space vehicle, it is reasonable that it should be tested in a vacuum. This gives more realistic thermal performance. It also protects the cell against atmospheric corrosion.

Originally, an 18-inch diameter bell jar vacuum system was used for testing the thermionic converter. This had a water cooled base and has been provided with internal electrical connections delivering up to 200 amperes at 18 volts ac and up to 5 amperes at 500 volts ac. Both optical pyrometers and noble metal thermocouples were used for measuring the temperature of different parts of the cell. The output current-voltage curve for the thermionic converter was monitored continuously with an oscilloscope, using a 60-cycle a-c sweep. The filament transformer supplying the 60-cycle sweep was capable of delivering 10 amperes at 6 volts rms.

Preliminary experiments in the bell jar system were difficult to interpret due to electrical interaction between the heater input circuit and the thermionic output circuit. This appeared to be mainly due to electrons from the heater filament

striking the heat radiator of the thermionic converter, which is in electrical contact with its anode. A second experimental difficulty was experienced in determining the cathode temperature by optical pyrometry. The source of bombarding electrons was a tungsten filament in close proximity to the cathode of the thermionic converter. The tungsten filament needed to be hot enough to emit a considerable flow of electrons, even for the initial experiments in which the cathode of the thermionic converter was at a relatively low temperature. Consequently, the brilliant light from the tungsten filament, reflected from the cathode, interfered with determination of the cathode temperature by optical pyrometry.

Both of these difficulties can be alleviated by using a higher voltage input circuit so that the electron bombardment current can be decreased. This reduces the electrical coupling and at the same time makes possible a smaller tungsten filament with reduced radiation. Both interferences can be further reduced by using a carefully designed electron gun in which the filament is removed from the immediate vicinity of the cathode, and in which the electron beam can be concentrated on the cathode, with relatively few electrons striking the anode circuit.

Arrangements were made, therefore, for intermittent use of a high voltage electron beam bombarder. This apparatus, shown in Figure 20, comprises a cubic vacuum chamber approximately 2 feet on a side with an electron gun mounted at the top. The gun will deliver up to 150 milliamperes of electrons at up to 20 kilovolts in a concentrated beam utilizing a three-phase full wave rectifier. The original circuit used to observe the current-voltage output curve is indicated in Figure 21. The anode was cooled by a radiator, but this had no separate heater to raise its temperature. The only way to get the anode to its proper operating temperature, therefore, was by heat radiated from the cathode.

Four cells were filled with barium and tested. In the first cell, thermionic emission from the cathode was observed, but the ceramic insulator reached such a high temperature that the brazing alloy melted and apparently vaporized. The second cell failed due to heat shock at the ceramic-to-metal seal.

These first experiments showed a need for several improvements:

a. The anode radiator needed a separate heater so that its temperature could be varied independently of the cathode temperature.

b. There was a tendency for the alumina ceramic insulator to get too hot.

c. The ceramic-to-metal bond needed to be strengthened.

d. There was still some interaction between the bombarder circuit and the cell output circuit.

The following steps were taken:

a. The 6-inch diameter radiator (Figures 22, 23) was provided with a 500-watt heater, and a 12-inch diameter radiator (Figure 24) was made and provided with a 1500-watt heater.

b. The anode was redesigned to give better thermal contact to the ceramic ring and to partially shield it from the cathode radiation.

c. New beryllium oxide ceramic rings were ordered, already metallized.

d. An electron shield was inserted between the electron gun and the anode-radiator assembly. When cathodo-luminescence of the beryllium oxide insulator still showed some electrons reaching it, an electron trap was added to the above mentioned shield.

e. A thermal shield was installed between the barium reservoir and the radiator.

f. The resistors used to measure the output current and to couple the sweep voltage were increased to 5 ohms and the maximum sweep voltage was raised by a factor of five. The changes are indicated in Figure 25.

After these changes had been made, the temperature distribution in the cell was much improved. The higher thermal conductivity of the beryllium oxide ceramic, with full thermal contact to the anode, resulted in much lower ceramic temperatures. The massive 12-inch diameter radiator with its 1500-watt heater made possible experiments with the radiator temperature at any value between 150 degrees C and 550 degrees C. The barium reservoir could be heated to 850 degrees C in the exposed portion of the tantalum tubulation, but the temperature at the top end of the tantalum tubulation was unknown, and at the lower cathode temperatures it is probable that barium condensed in the upper part of the tantalum tubulation thus exerting an indeterminate sublimation pressure. Several reservoir heaters were burned out attempting to get heat up to this top part of the reservoir.

Cells No. 3 and 4, both with beryllium oxide insulation, gave the most satisfactory data. The electron bombardment equipment was used for other projects also, so was available only on scheduled days. It proved to be an excellent method of heating except for a rather poorly regulated beam current. As the beam was operated, say with 30 milliamperes at 15 kilovolts, it would often change up or down by a factor of one and a half, without warning. With more time available, the current could have been regulated automatically, or an extra man could have been used to give his attention exclusively to beam control. During a run, two men were normally

kept busy measuring the cathode, anode, and reservoir temperatures, taking photographs of the oscilloscope trace, checking on stray electron currents, condition of vacuum, etc.

Over 100 current-voltage curves were recorded. Sixty four of these curves are shown in Figures 26 to 33, in the order in which they were recorded. The conditions under which the different records were made are given in Tables 4 and 5. It should be noted that the temperatures in these tables are estimates, partly because they were often changing rapidly and the rate of recording data was limited. Also, of course, a particular current-voltage curve has meaning only in consideration of its immediate past history. The most interesting curves with each cell were taken after the barium reservoir heater had burned out.

Effects due to slow drift of the oscilloscope d-c amplifiers were eliminated by occasional removal of the anode connection and manual centering. The current zero positions are usually self evident in the oscilloscope traces, since thermionic current is always recorded upward, and is absent in the negative direction. In the case of Figure 31d, however, there appeared to be a small current in the "wrong" direction due to very close spacing or slight "metallic" contact. In several cases the zero was intentionally displaced (as in Figure 32e) to bring the upper part of the trace into view. Unfortunately, the reticule lines were in most cases under-exposed. The currents and voltages corresponding to a single vertical and horizontal division are recorded in Tables 4 and 5. For the heavier cell currents horizontal deflection is markedly reduced (Figures 30g, 31d). For these heavier currents it appears that lower load and coupling resistors would have been better.

Referring first to Figure 26a and b, which have a vertical gain of 0.4 amp/div, it can be seen that the maximum current is 1.2 amperes. This is believed to be due to a discharge in the barium vapor. The barium reservoir temperature was 740 degrees C, but the radiator temperature was only 303 degrees C. Breakdown occurs at approximately 4 volts positive, with the current apparently rising to 1.2 amperes and the voltage dropping to 2.5 volts. Careful examination of the original photograph discloses that the current assumes at least three values for the same voltage across the cell, and that the voltage decreases simultaneously with an increase of current. Similar discharges are recorded in Figures 26c, d, 27g, 28a, b, c, d, and 29 f.

Figure 30b shows an instance of saturated emission, where the current remains nearly constant at 10 milliamperes while the voltage varies from 5 to 14 volts. The ability of the cell to stand a higher forward voltage in this case without breakdown is presumably due to the lower radiator temperature (171 degrees C) which implies a lower temperature of the anode surface. Figure 32h appears to show saturated emission of 140 milliamperes even at a back bias of 0.7 volts. Since in this case the radiator temperature was 556 degrees C and the reservoir temperature was 617 degrees C, it might be assumed that the barium pressure was quite high. Unfortunately, the recorded reservoir and radiator temperatures were not always good indications of the barium pressure. As a compromise, the thermocouple used to indicate the reservoir temperature had been placed on the tantalum tubulation, just below the radiator. In Figure 32h, the coolest part of the tubulation (where the barium

Table 4

Data for Figures 26 - 29

Figure	Cell	Date	Time	Cathode Temp (°C)	Radiator Temp (°C)	Reservoir Temp (°C)	Vert Gain (amps/div)	Horiz Gain (volts/div)
26a	3	5-18-62	3:37P	1115	303	740	0.40	5
26b	3		3:38P	1115	303	735	0.40	5
26c	3		3:47P	1115	303	325	0.40	5
26d	3		3:53P	1115	288	266	0.40	5
26e	3	5-29-62	7:53P	1070	65	352	0.01	1
26f	3		7:54P	1070	65	354	0.01	1
26g	3		8:42P	1076	135	860	0.04	2
26h	3		8:43P	1076	136	855	0.20	5
27a	3		8:51P	1076	147	635	0.04	2
27b	3		9:10P	1030	154	428	0.04	2
27c	3		9:11P	1000	155	395	0.04	2
27d	3		9:13P	900	156	391	0.04	2
27e	3		9:30P	1025	158	350	0.10	5
27f	3		9:31P	1025	158	350	0.10	5
27g	3		9:33P	1175	161	349	0.10	5
27h								
28a	3		9:38P	1175	161	330	0.10	5
28b	3		9:39P	900	161	329	0.10	5
28c	3		9:42P	1100	161	328	0.10	5
28d	3		9:43P	900	161	327	0.10	5
28e	3		9:47P	1160	161	326	0.04	2
28f	3	5-30-62	9:50A	(anode disconnected)			0.04	2
28g	4		9:32A	1060	62	352	0.001	2
28h	4		9:33A	1060	63	353	0.01	2
29a	4		10:15A	1100	130	415	0.002	2
29b	4		10:16A	1100	131	420	0.002	2
29c	4		10:17A	1100	134	424	0.010	2
29d	4		10:32A	1100	148	430	0.010	2
29e	4		10:42A	1125	154	530	0.010	2
29f	4		10:45A	1125	160	602	0.100	2
29g	4		10:51A	1125	165	712	0.020	1
29h	4		10:55A	975	168	730	0.004	0.5

Table 5

Data for Figures 30 - 33

Figure	Cell	Date	Time	Cathode Temp (°C)	Radiator Temp (°C)	Reservoir Temp (°C)	Vert Gain (amps/div)	Horiz Gain (volts/div)
30a	4	5-30-62	11:20A	800	170	842	0.02	5.0
30b	4		11:25A	800	171	843	0.02	5.0
30c	4		11:30A	1025	172	882	0.02	2.0
30d	4		11:37A	1025	177	886	0.02	2.0
30e	4		11:42A	1300	180	840	0.04	2.0
30f	4		11:43A	1300	183	800	0.04	2.0
30g	4		11:46A	1300	185	770	0.04	2.0
30h	4		11:47A	(anode disconnected)			0.04	2.0
31a	4		1:12P	1400	470	560	0.20	0.5
31b	4		1:13P	1400	490	561	0.20	0.5
31c	4		1:14P	1475	500	580	0.20	0.5
31d	4		1:15P	1475	515	590	0.20	0.5
31e	4		1:17P	1475	532	607	0.20	0.5
31f	4		1:18P	1475	540	608	0.20	0.5
31g	4		1:19P	1500	540	610	0.20	0.5
31h	4		1:20P	1500	590	610	0.10	0.5
32a	4		1:24P	1525	542	612	0.04	0.5
32b	4		1:25P	1525	544	613	0.04	0.5
32c	4		1:26P	1525	546	614	0.04	0.5
32d	4		1:27P	1525	548	615	0.04	0.5
32e	4		1:31P	1550	550	616	0.04	0.5
32f	4		1:34P	1575	556	617	0.04	0.5
32g	4		1:39P	1575	556	617	0.10	0.5
32h	4		1:44P	1575	556	617	0.10	0.5
33a	4		1:46P	1150	550	570	0.10	0.5
33b	4		1:47P	1150	530	530	0.10	0.5
33c	4		1:50P	900	490	510	0.01	1.0
33d	4		1:51P	900	470	500	0.01	1.0
33e	4		1:59P	850	331	430	0.01	1.0
33f	4		1:60P	850	325	400	0.01	1.0
33g	4		2:04P	850	320	370	0.0004	1.0
33h	4		2:06P	500	315	340	0.0004	1.0

condenses) was probably in the lower end of the tubulation, for the reservoir heater had burned out at 11:40 AM, and the lower end of the tubulation presumably cooled steadily thereafter. On the other hand, the radiator heater was turned on at 12:44 PM, and the cathode temperature also was raised, with the result that the thermocouple used to indicate the reservoir temperature gave a considerably higher reading at 1:44 PM, (when curve 32h was recorded) than at 12:44 PM when the radiator heater was turned on. Ideally, the coolest part of the reservoir, where the barium condenses, should always be the low part of the tubulation. Furthermore, the thermal coupling to this point from the cathode and anode should be minimized, and the thermocouple used to record the reservoir temperature should be placed at this low point of the tubulation.

The magnitude of spurious signal in the thermionic output circuit is estimated from Figures 33h to be approximately 0.1 milliampere. This 60-cycle signal is primarily due to pickup from the radiator and reservoir heater circuits. The cathode heater circuit was rectified three phase, unfiltered. Thus pickup from this circuit was easily recognized when it was visible at the high oscilloscope gains. It could be eliminated when desired, by momentarily cutting off the high voltage on the electron beam.

On several occasions several oscilloscope traces were photographed on the same film, as the cathode was rapidly cooled or heated. Thus in Figure 33 f the electron beam heating had been shut off and as the cathode cooled about 10 traces were photographed, with the first 7 being at 5-second intervals.

4.1 Condensation and Sublimation of Barium at the Anode Surface

A most convenient method for analyzing vacuum thermionic currents in the presence of space change has been worked out by Webster[3]. Detailed curves from this work were kindly supplied to the writer by Dr. Webster. Two sets of curves from Webster's paper are reproduced in Figures 34 and 35. In Figure 34 the sign of the normalized voltage is reversed from that used by Webster. Figure 34 shows a set of normalized current versus voltage curves for different values of a dimensionless parameter R. Both the current and the parameter R are normalized with respect to the saturated thermionic emission. Unfortunately, in many cases saturated emission could not be measured because electrical discharge in the barium vapor limited the positive voltage that could be applied to the anode. However, essentially saturated emission is shown in Figures 30b, 32g, h, and 33 b, g. Because of the effect of barium pressure on the cathode work function, the saturated emission varied markedly with the barium pressure.

In comparing the oscilloscope traces to the theoretical curves in Figure 34, it is to be noted that in both cases the thermionic current is plotted upward. A positive voltage applied to the anode is shown to the right in each case, (the cathode being grounded as shown in Figures 21 and 25). In Figure 34 the anode voltage is shifted by an amount equal to the contact potential between anode and cathode.

In our experiments, the contact potential was in many cases unknown, or unevaluated. Webster suggests that for vacuum converters, the contact potential can be obtained by an exact comparison between the experimental curves and his theoretical curves. In the presence of barium vapor an exact comparison is not always possible, for electrical discharge can prevent observation of the complete thermionic curve to the limit of saturated emission. Furthermore, when barium is built up on the anode, the effective area of close spacing may be unknown - particularly for our small test models. With larger test models and more uniform temperature distribution, as in Figure 7, it would be possible to estimate the effective area with a reduced percentage error.

In spite of the above mentioned uncertainties, however, one can assign definite upper limits to the thermionic current that can flow with no barium in the anode-cathode space. As shown in Figures 9 and 10, the spacing designed into the test model is 0.007 inch or 0.018 cm. The maximum possible area is 0.267 square inch or 1.72 square centimeters. The temperature was usually less than 1200 degrees C, so we may take a nominal value of 1227 degrees C = 1600 degrees K. Figure 35, taken from Webster, gives values of R/J_S as a function of temperature "T" and spacing "d", but it does not extend up to our spacing of 0.007 inch. We calculate that R/J_S is equal to 4260 cm^2/amp at 1600 degrees K and 6370 cm^2/amp at 1225 degrees K.

The actual current with a spacing of 0.007 inch depends somewhat on the saturated emission. In order to use Webster's curve for his maximum value of R = 5000, we chose first a value of 1.17 ampere/cm^2 for the saturated emission. Reading off Webster's curve for R = 5000 and $\phi_p - \phi_K = 0$, we find $J/J_S = 0.0125$, so J = 0.0145 ampere/cm^2. If we had taken $J_S = 0.47$ ampere, then we would have found R = 2000, $J/J_S = 0.29$, and a slightly lower value J = 13.5 milliamperes/cm^2. If we had instead calculated for the lower temperature T = 1225 degrees K, and taken $J_S = 0.786$ ampere/cm^2, then we would again obtain R = 5000, so that for $\phi_p - \phi_K = 0$, J = 9.8 milliamperes/cm^2. Thus, even for the higher temperature T = 1600 degrees K, the space charge limited current for a spacing of 0.007 inch should not exceed 17 milliamperes/cm^2. Although the contact potential is not known, the quantity $\phi_p - \phi_K = V_a - V_c - (\phi_a - \phi_c)$ is in all probability negative for the peak current in Figure 31e, for which $V_c = 0$, $V_a = -0.7$ volts. Even if we assume that the value of $\phi_c - \phi_a$ can be as high as 0.85 volt, then for our measured value $V_a - V_c = -0.7$ volt, the value of $\phi_p - \phi_K$ would be + 0.15 volts. This is only slightly greater than one unit of the normalized voltage $(\phi_p - \phi_K)e/kT$ (which is equivalent to 0.138 volt at 1600 degrees K), so that even for this extreme case the current in our test model could not exceed 40 milliamperes with a spacing of 0.007 inch.

Currents much in excess of this calculated value are actually recorded in Figures 31e and 33a. For example, in Figure 31d, the cell produced a current of 0.48 ampere against a decelerating (i.e., negative) anode potential of 0.7 volt. This is 12 times the space-charge limited current calculated for $\phi_c - \phi_a = 0.85$ volt and for an area of 1.72 cm^2 and a spacing of 0.007 inch. Observation of these relatively high thermionic currents constitutes a proof that barium is indeed depositing on the anode surface and closing down the gap.

Immediately preceding these high current observations, a metallic contact had existed in the cell intermittently for some 52 minutes. The development of the ohms-law type of current-voltage relation into a thermionic current-voltage curve is recorded in Figures 31a, b, c, and d. No perfectly straight line through the origin was recorded at this time, because these "resistors" had been seen before and were not deemed of sufficient interest to record. However, Figure 30g shows a short circuit which had existed almost continuously in the cell for the preceding 34 minutes. (Figure 30h was taken with the anode disconnected, to show a slight misorientation of the trace with respect to the reticule). The short circuit developed with an anode temperature near 190 degrees C and a cathode temperature in the neighborhood of 1025 degrees C. The cathode was then heated to 1310 degrees C, at which temperature the short disappeared momentarily, then reappeared. Thirty four minutes after the short first appeared, when the cathode temperature had risen to 1450 degrees C, the short was converted to an ohmic resistor which varied from 0.25 to 0.5 ohm. Twenty four minutes later, 500 watts were applied to the 12-inch diameter radiator heater. Three minutes later, another 1000 watts were applied. Finally, 52 minutes after the short turned to a resistor, at a radiator temperature of 500 degrees C, the resistor began to turn into a thermionic current-voltage curve. Figure 31a, b, c, and d, were recorded during the next 5 minutes.

It was desirable to cycle from large to small spacing and back again several times. Unfortunately, in each of the last three runs the experiment was terminated by burn-out of the barium reservoir heater. A high reservoir heat was apparently needed to drive barium out of the top part of the tantalum tubulation, which was difficult to heat with the reservoir heater. A new anode design, with this part of the tubulation more accessible, is suggested in Section 5.0.

4.2 Activation of the Cathode by Sublimation of Barium

In the experiments of May 11 and May 18, 1962, with relatively low barium pressures, it was noticed that shutting off the electron beam heater often resulted in a transient increase of thermionic current, followed a few seconds later by a decrease as the cathode cooled toward room temperature. This type of experiment was repeated many times, changing the cathode temperature gradually or suddenly, and there was no doubt that the lower cathode temperatures were allowing more barium atoms to deposit on the cathode surface and thus to lower its work function. From the data in Table 1, barium at a pressure of 10^{-5} mm can deposit on a surface at the rate of 0.045 microns/minute or 7.5×10^{-8} cm/sec. Since a large fraction of a monolayer could be observed to form in less than 10 seconds, the barium pressure must have been at least 10^{-7} mm. Actually, at a reservoir temperature of 418 degrees C, the pressure was in the neighborhood of 10^{-5} mm, so that the time for a rise in emission must have been determined mainly by the rate of cooling of the cathode.

For pressures below 10^{-7} mm, barium pressure could be estimated by its rate of deposition on the cathode. Above 10^{-7} mm, the pressure could be estimated by its rate of condensation on the anode.

After these initial observations, some attempt was made to operate on the peak of the Taylor-Langmiur S-curve for barium. However, in later experiments, when barium began to build up on the anode, the transient response to a sudden change of cathode temperature became more complicated. When the anode surface was the coolest part of the enclosure, rather than the barium reservoir, then a sudden drop of cathode temperature had the additional effect of lowering the barium pressure. Thus in the later experiments, with higher barium pressures, the most common result of a drop in cathode temperature was a consequent drop in cathode emission.

5.0 SUGGESTED IMPROVEMENTS IN TEST MODEL CONVERTER

The model converters tested on this contract did not always have a well-defined area of lowest temperature where the barium would build up. Furthermore, sometimes the coolest part of the barium reservoir was the top part of the tantalum tubulation; this was not adequately heated by the reservoir heater, nor its temperature properly determined by the reservoir thermocouple.

Moreover, changes of cathode temperature had marked effects on the barium pressure. In order to perform clear cut experimentation and interpretation, it is desirable to be able to maintain a barium reservoir pressure almost independent of the cathode and anode temperatures.

An anode design capable of giving a more clear cut demonstration of the subliming metal principle, with automatic regulation of the anode-cathode spacing, is indicated in Figure 36. This model has both the outermost and innermost part of the anode surface undercut to prevent easy escape of the heat received from the cathode. Thus the temperature of the undercut areas rises and prevents condensation of barium in any place except where it is desired; i.e., in the immediate vicinity of the cathode. With this design, the top part of the tantalum tubulation is more accessible than in the anode of Figure 10. To ensure that barium does not condense in the top part of the tantalum tubulation, it can be surrounded with highly insulating, laminar-type insulation, are even heated by a separate small heater. In addition, a constriction can be inserted part way down inside the tubulation, which will tend to confine radiation from the cathode to the upper part of the tantalum tubulation and thus keep it hot and the lower end of the tubulation cool.

In this way the coldest part of the barium reservoir will definitely be the lower part of the tantalum tubulation, which is thermally decoupled from the anode and cathode, where its temperature can be controlled at will by the reservoir heater and where its temperature can be properly determined by the reservoir thermocouple.

6.0 SUMMARY AND CONCLUSION

This report gives the theory of the subliming metal thermionic converter and describes a converter which will maintain high efficiency for long periods of time at elevated temperatures. It discusses both steady-state and transient temperature

distributions, together with the mechanisms for automatically regulating the anode-cathode spacing.

The test models are described, with details of the assembly techniques of welding, brazing, filling with subliming metal, pumping and sealing-off. Methods of testing for barium corrosion are described, together with the results of testing for several days at temperatures above 700 degrees C.

Observations on two test models are reported. Starting with an anode-cathode spacing of 0.007 inch, and a space-charge limited current of a few milliamperes, barium was driven into the cell until the thermionic current increased to nearly one-half ampere against a back bias of 0.7 volt. This current was 12 times higher than the highest possible space-charge limited current for the original spacing of 0.007 inch.

An increase in cathode emission was observed, due to activation of the cathode by a thin film of barium atoms. The work function was materially changed in a fraction of a second by changing the cathode temperature, and the peak of the Taylor-Langmuir S-curve for barium could be repeatedly traversed.

Driving the barium out of the tantalum tubulation proved to be unexpectedly difficult, so that optimum conditions of operation could not be investigated systematically. The difficulty is believed to be due to a tendency for barium to condense at the top end of the tantalum tubulation. This can be remedied by a simple modification of the design. In addition, it is desirable to make larger test models, which will achieve better regulation and higher efficiency.

Change of the anode-cathode spacing by build-up of barium on the anode has been conclusively demonstrated. Indications from this investigation are that the subliming anode thermionic converter has a high potential as a space power supply unit. It remains to be demonstrated that the converter can achieve and maintain high efficiency for long periods of time.

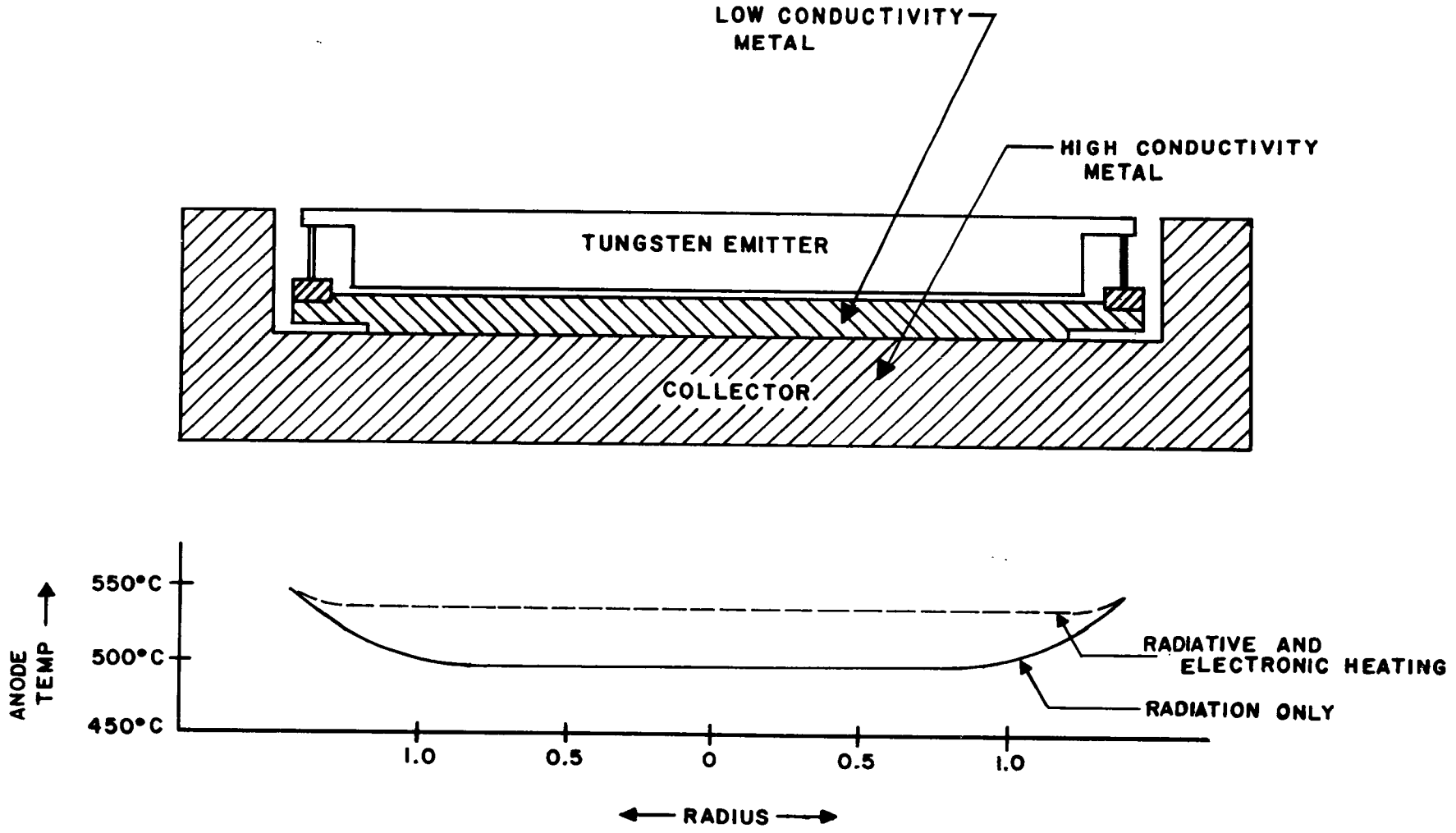

Fig. 1 - Parallel Plane Thermionic Converter with Decoupling Layer of Low Thermal Conductivity Metal

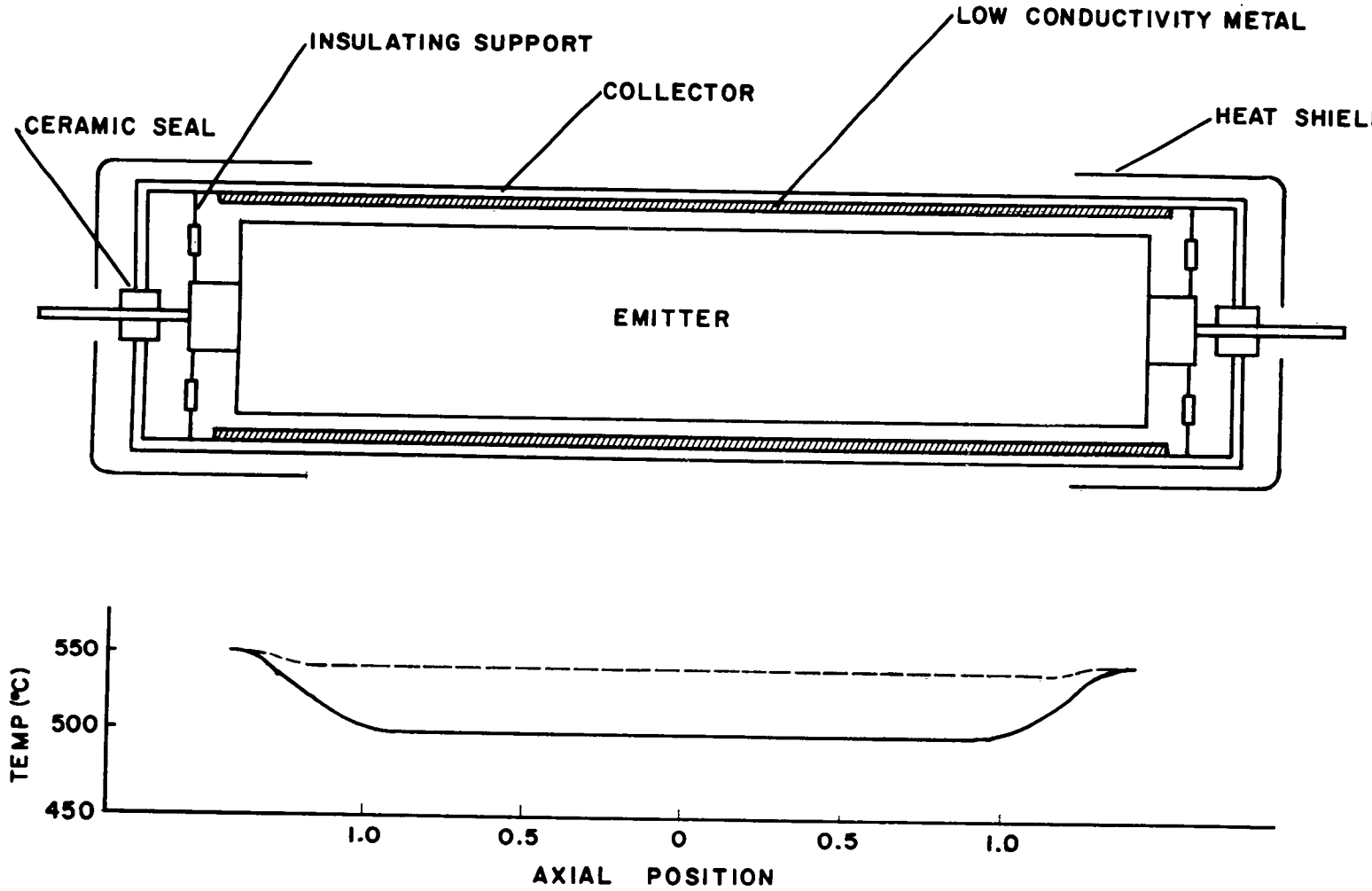

Fig. 2 - Cylindrical Thermionic Converter with Decoupling Layer of Low Thermal Conductivity Metal

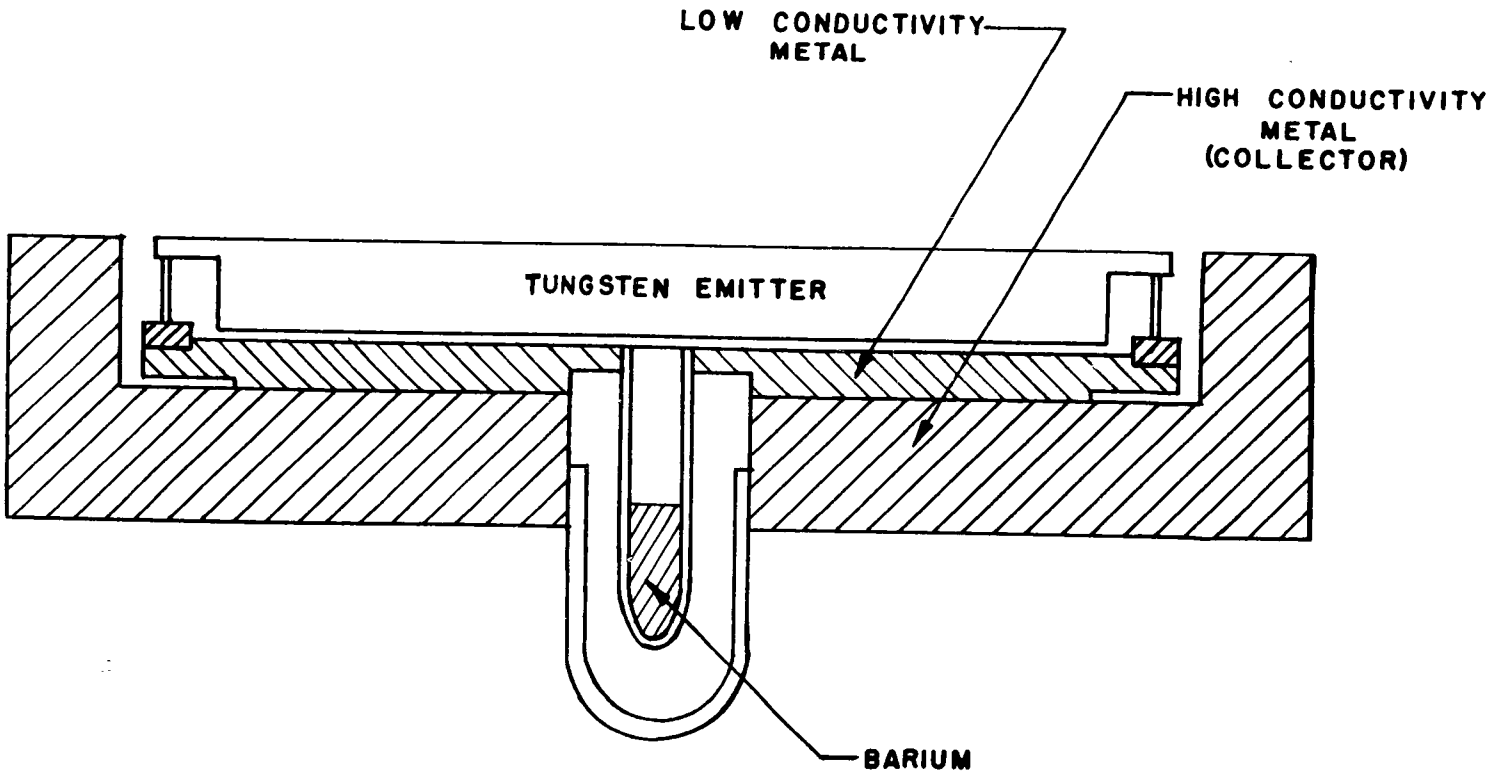

Fig. 3 - Thermionic Converter with Central Reservoir of Subliming Metal

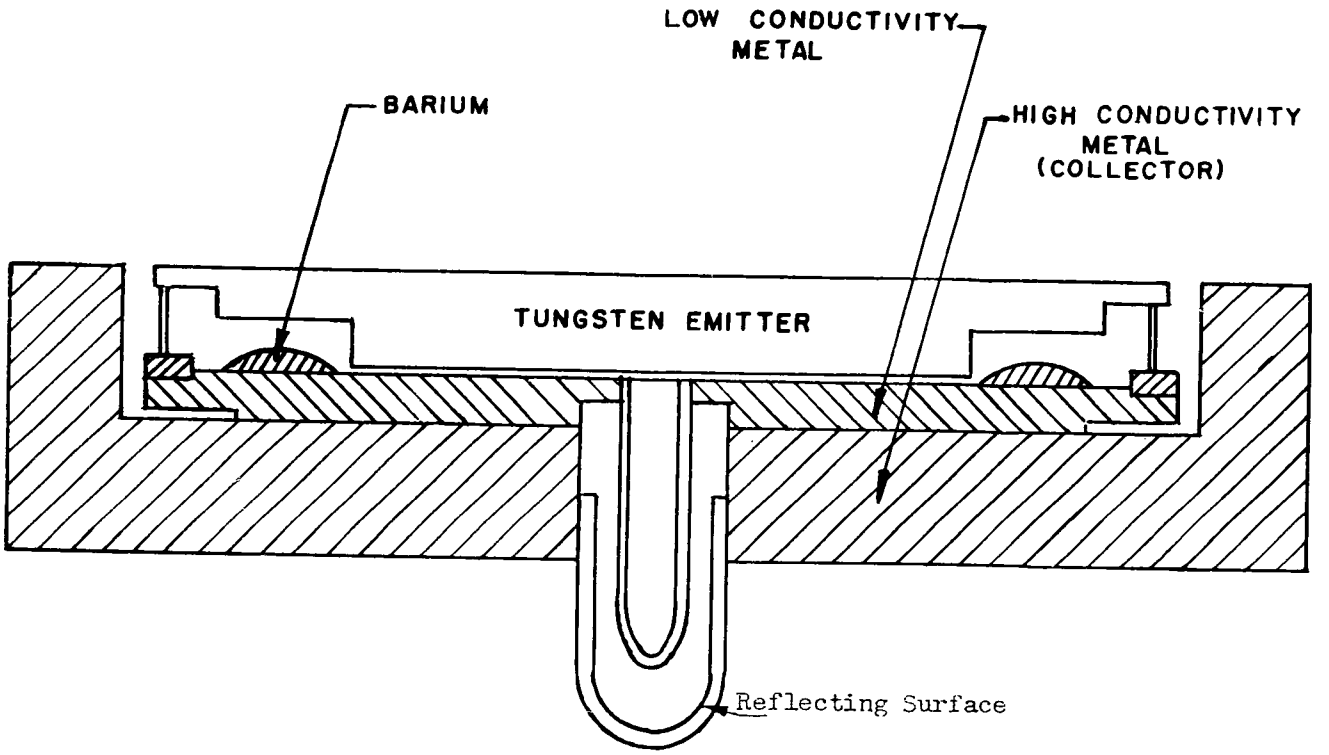

Fig. 4 - Thermionic Converter with Peripheral Reservoir of Subliming Metal

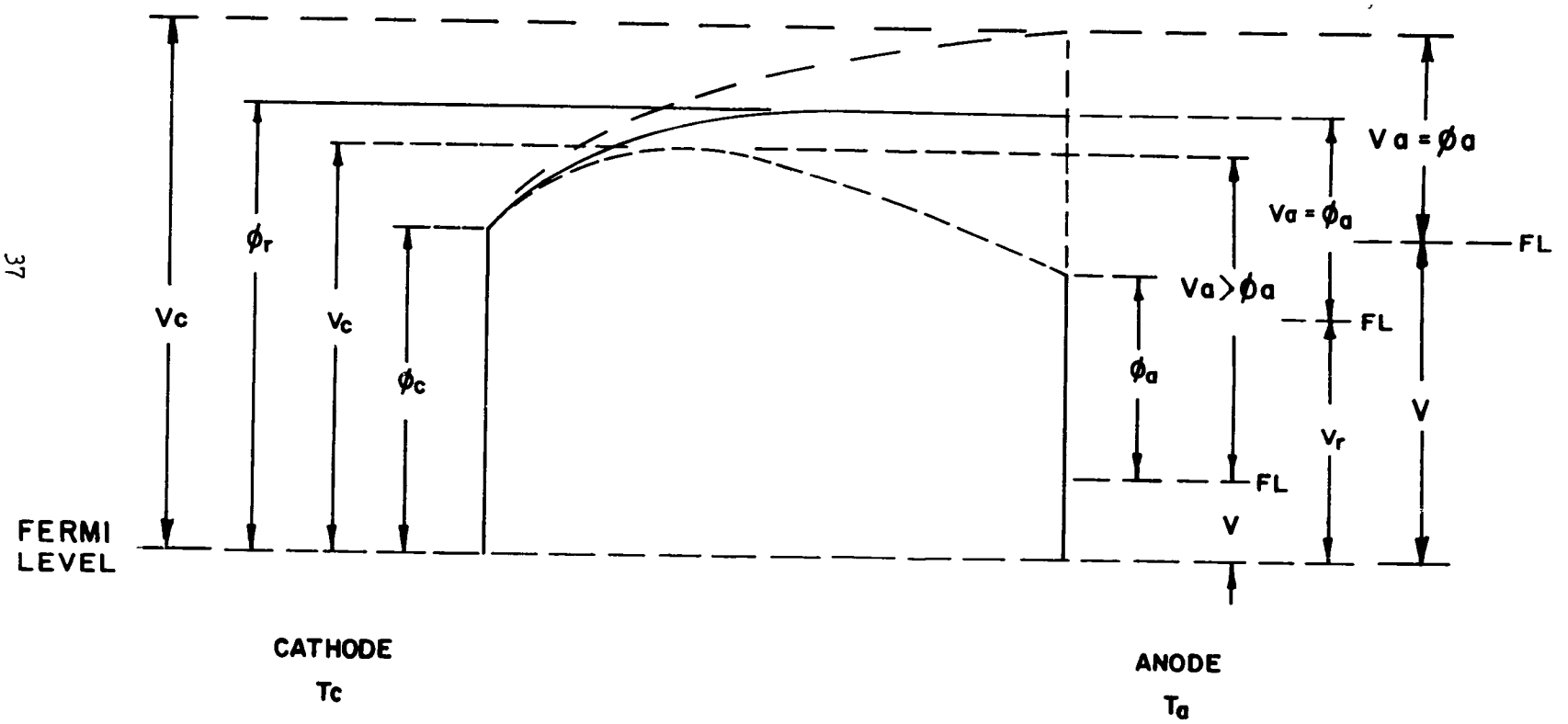

Fig. 5 - Electron Energy Level Diagram for Thermionic Diode

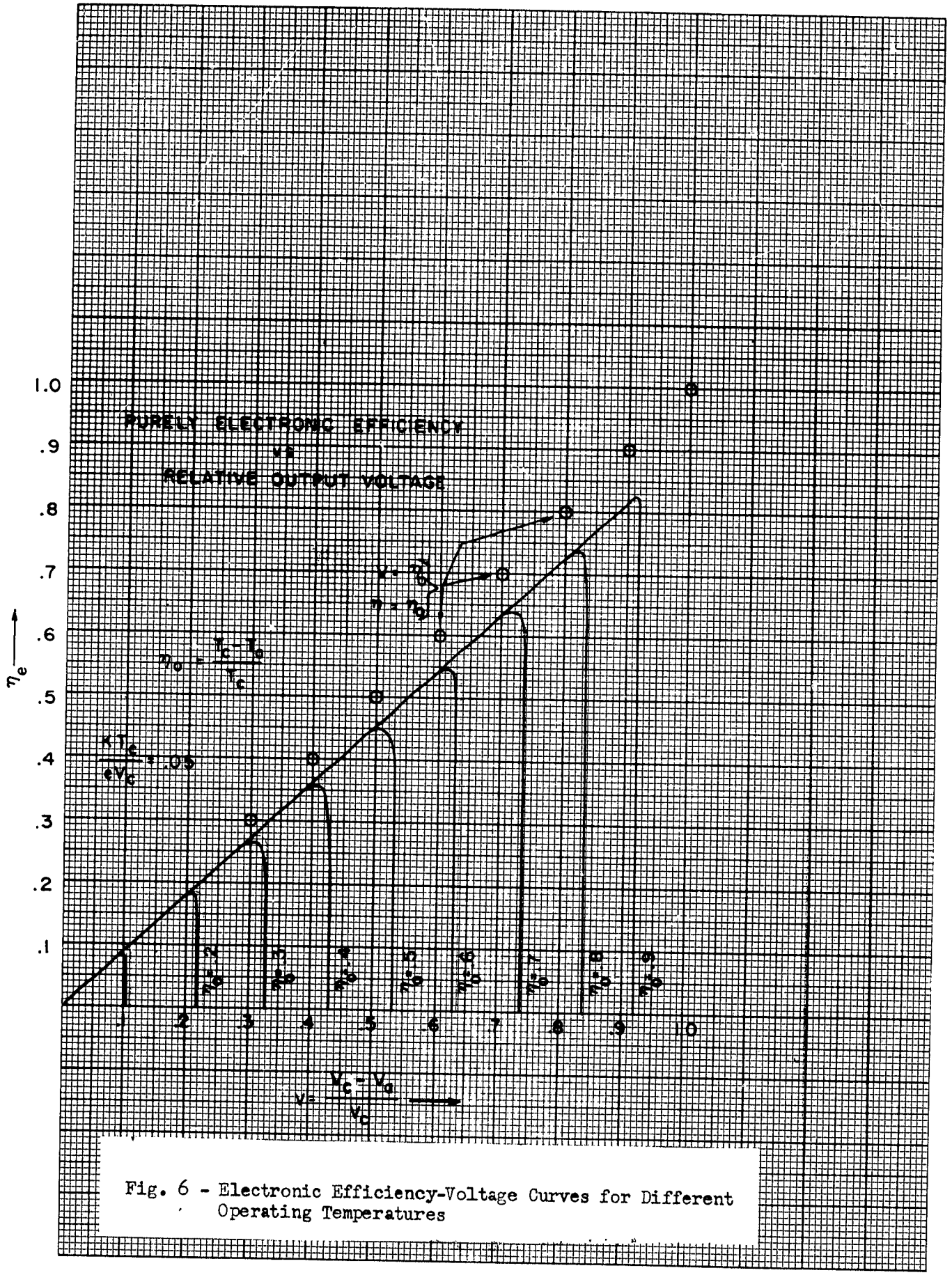

Fig. 6 - Electronic Efficiency-Voltage Curves for Different Operating Temperatures

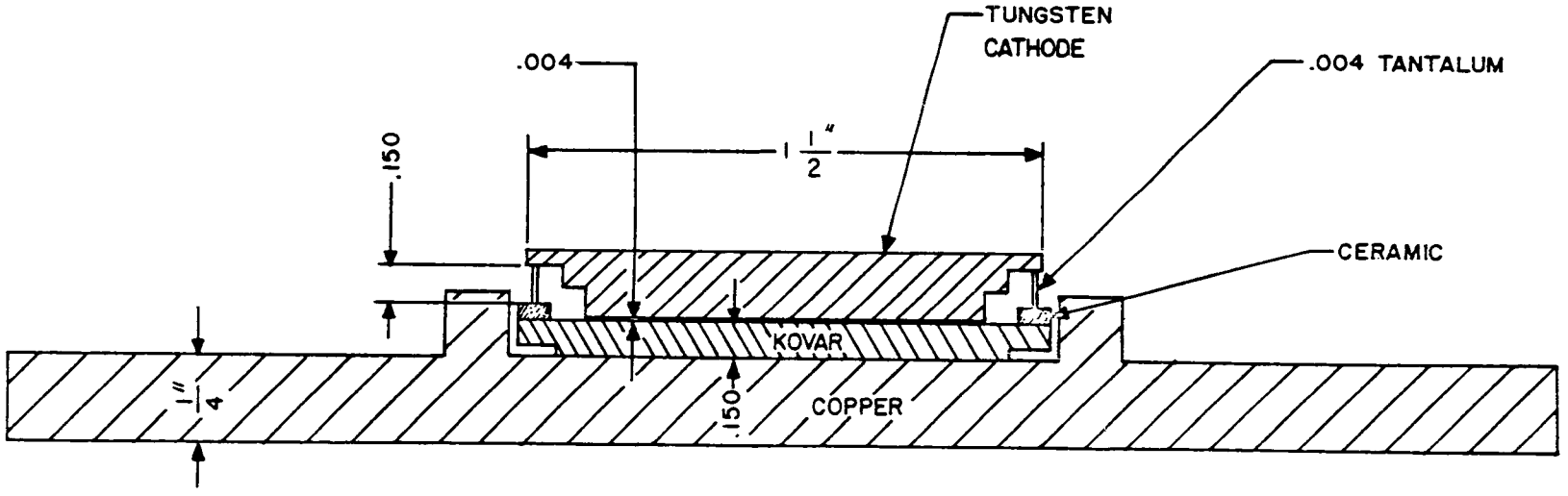

Figure 7 Thermionic Converter with Extended Anode for Radiation of Heat

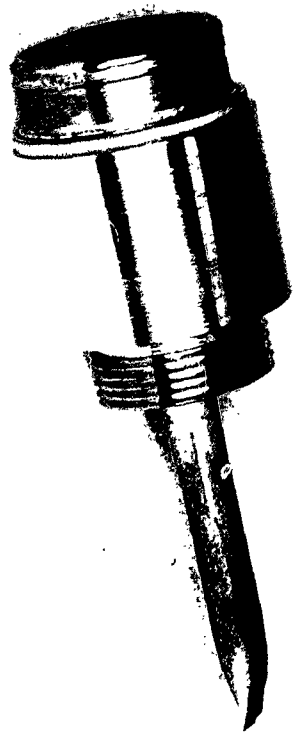

Fig. 8 - Test Model of Subliming Metal Thermionic Converter

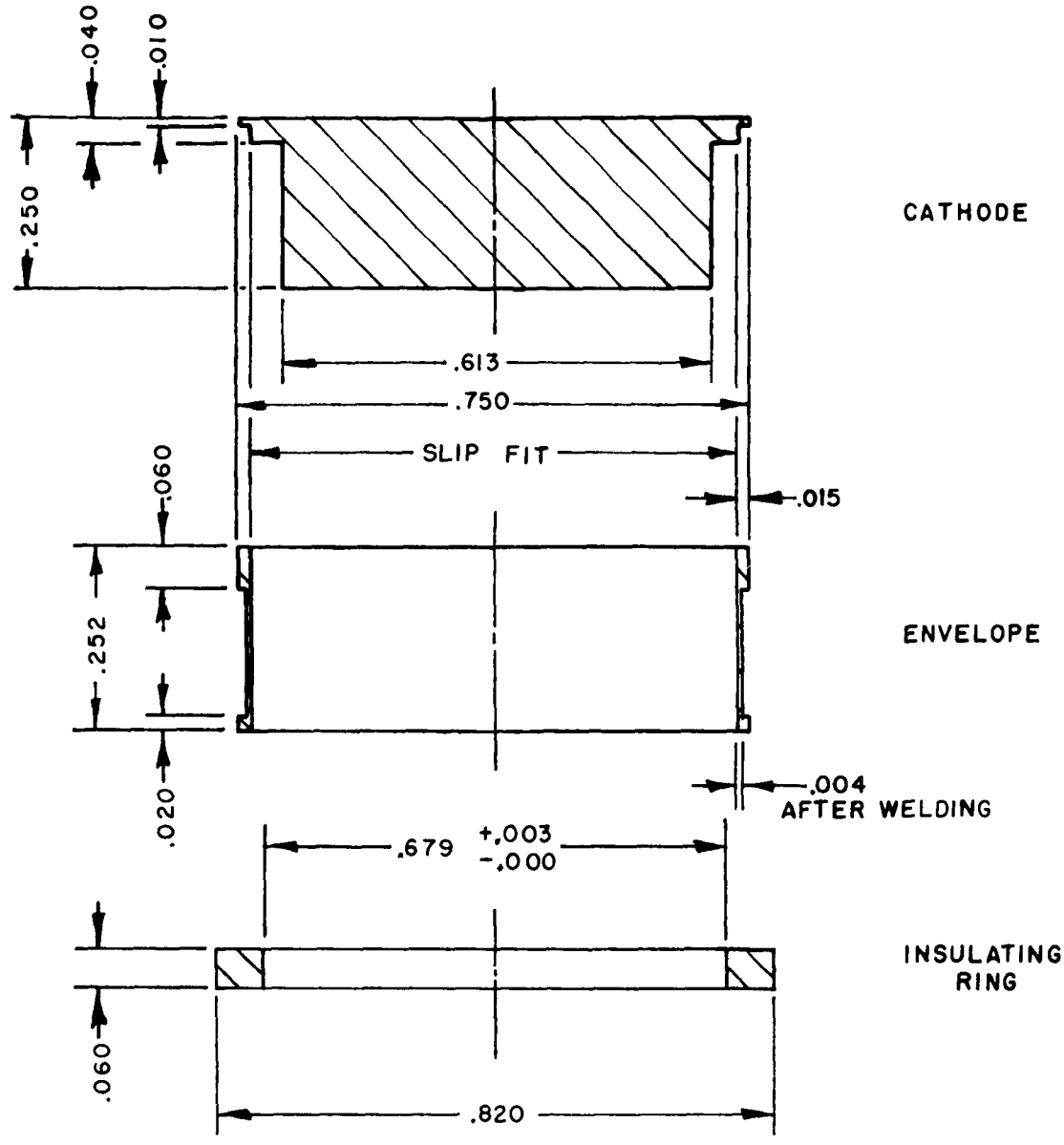

Fig. 9 - Cathode, Tantalum Envelope, and BeO Ceramic Insulator for Test Model

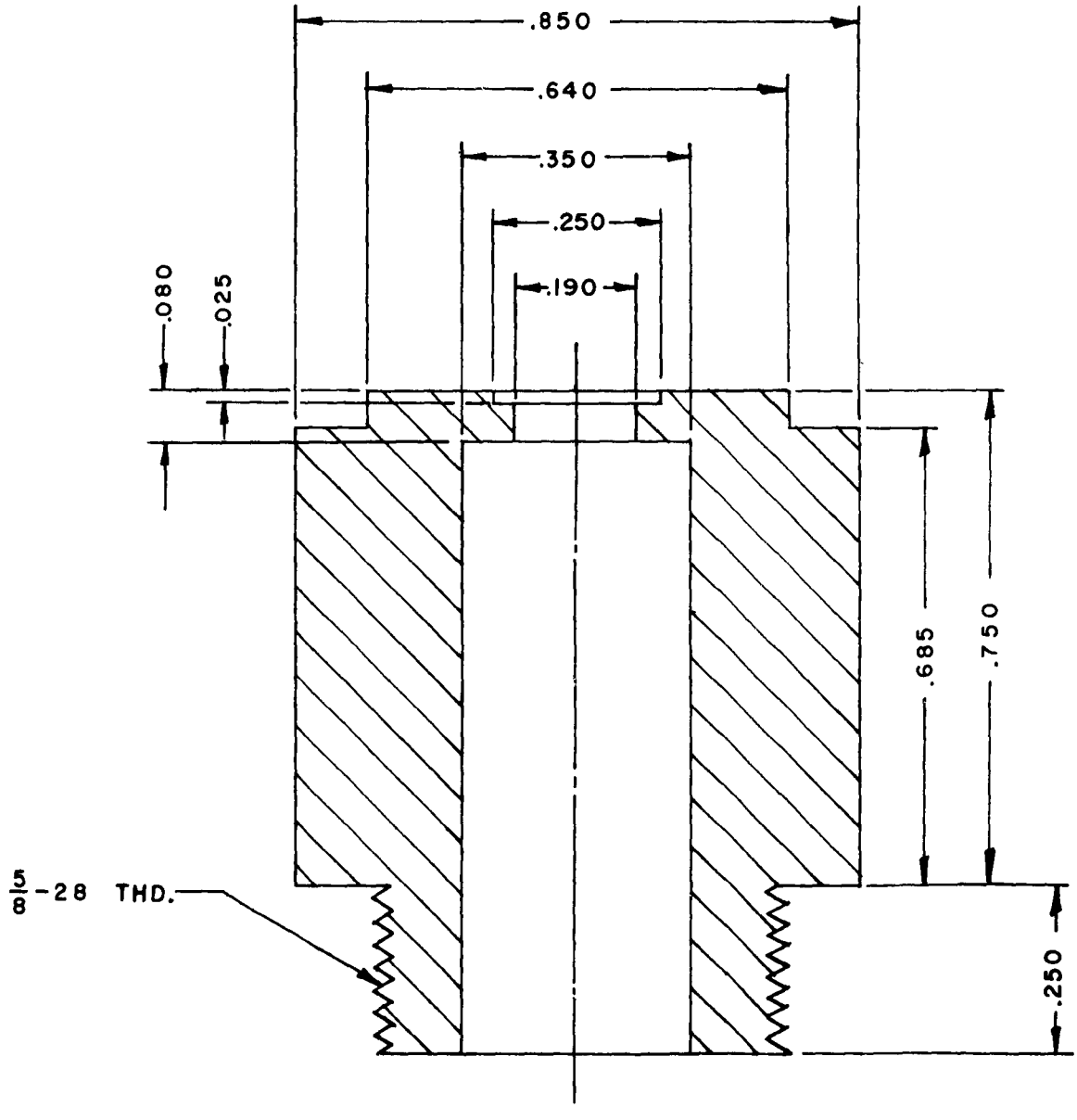

Fig. 10 - Anode for Test Model

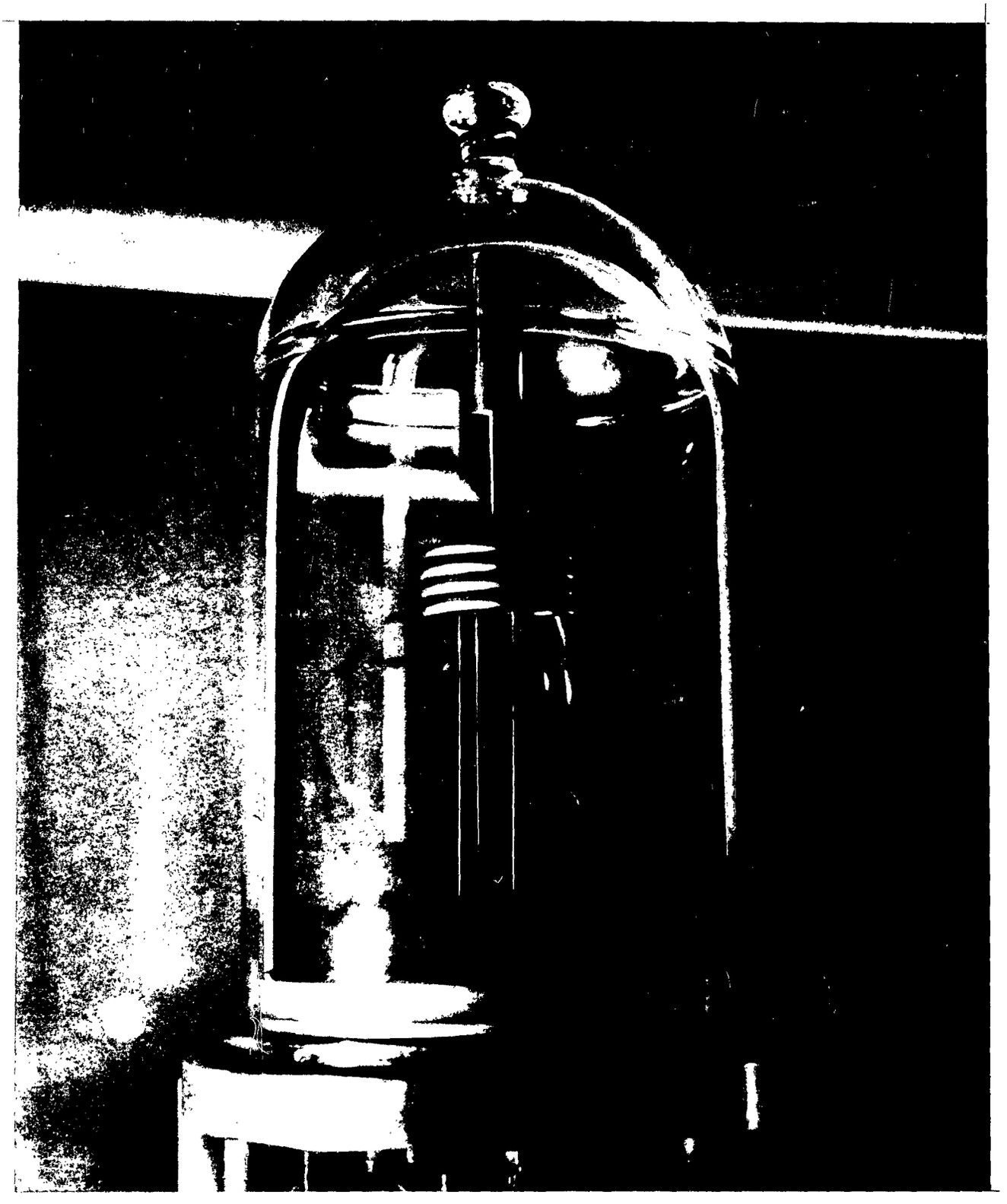

Fig. 11 - Vacuum Brazing System

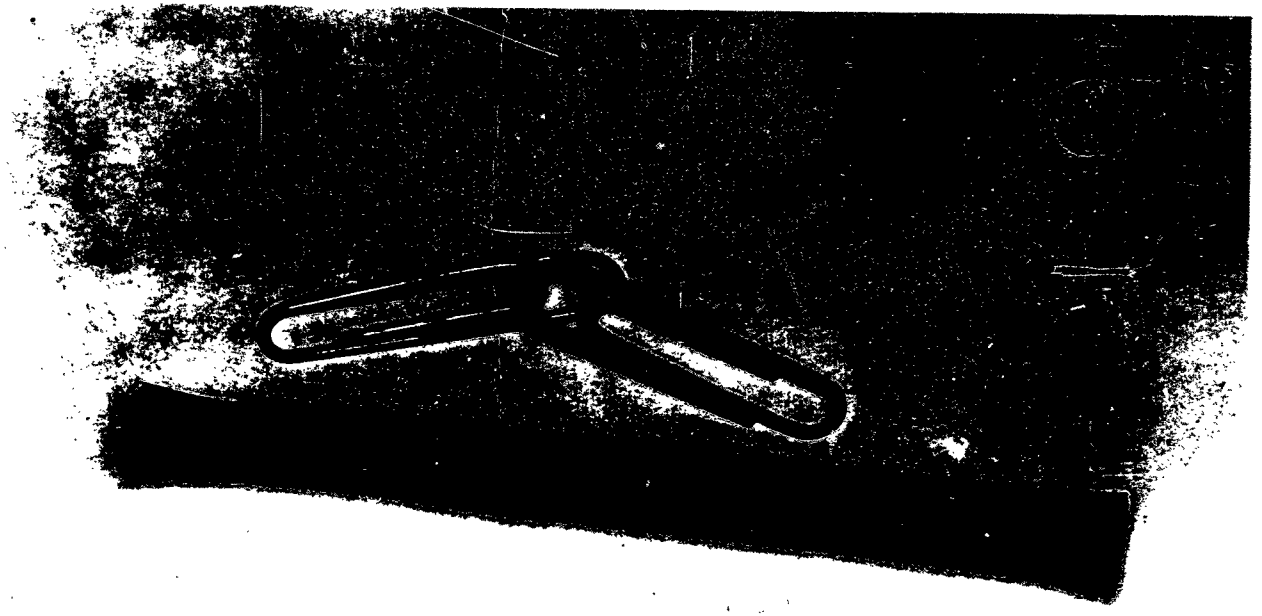

Fig. 12 - Tantalum Tube for Testing Materials with Hot Barium

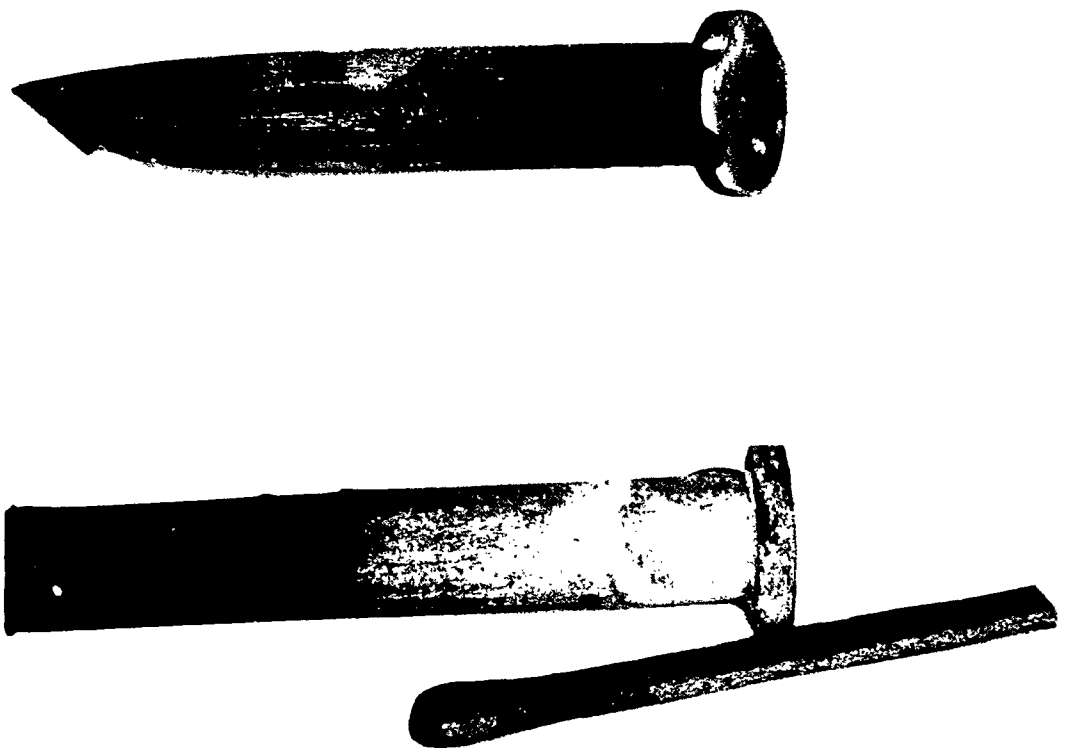

Fig. 13 - Test of Brazing Alloy

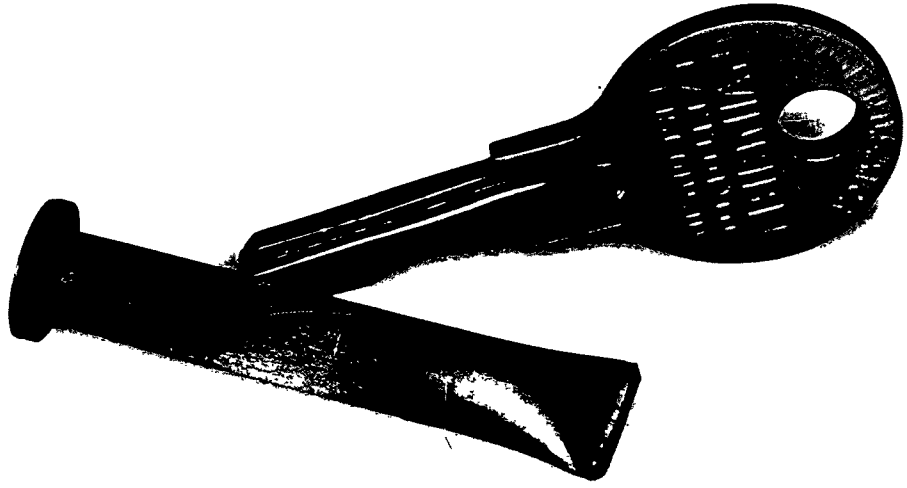

Fig. 14 - Two-Electrode Cell for Materials Test

Fig. 15 - Two-Electrode Test Cell

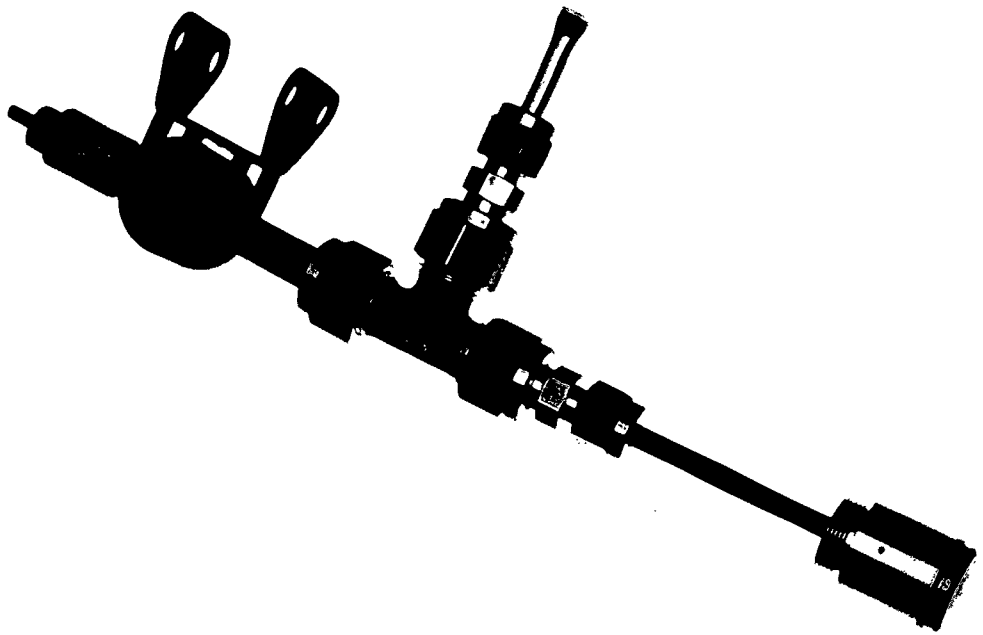

Fig. 16 - System for Filling, Pumping, and Sealing-Off Test Models

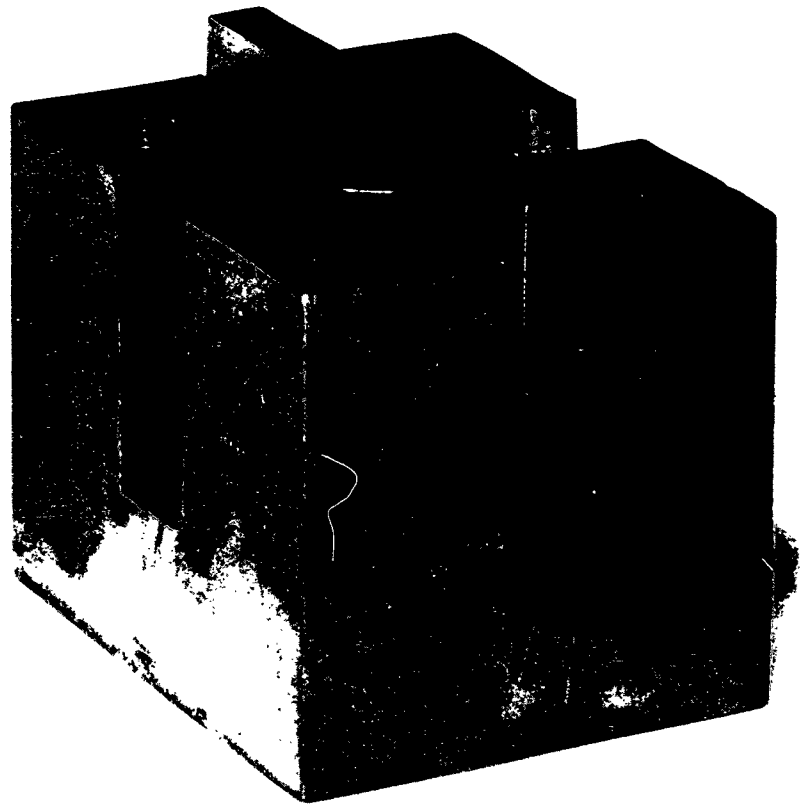

Fig. 17 - Jig For Pinching-Off Tantalum Tubing

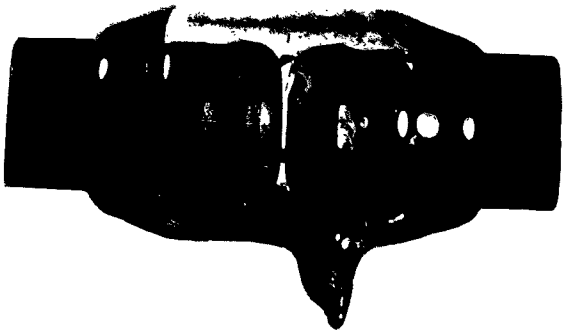

Fig. 18 - Low Temperature Test Cell for Observations on Subliming Cadmium

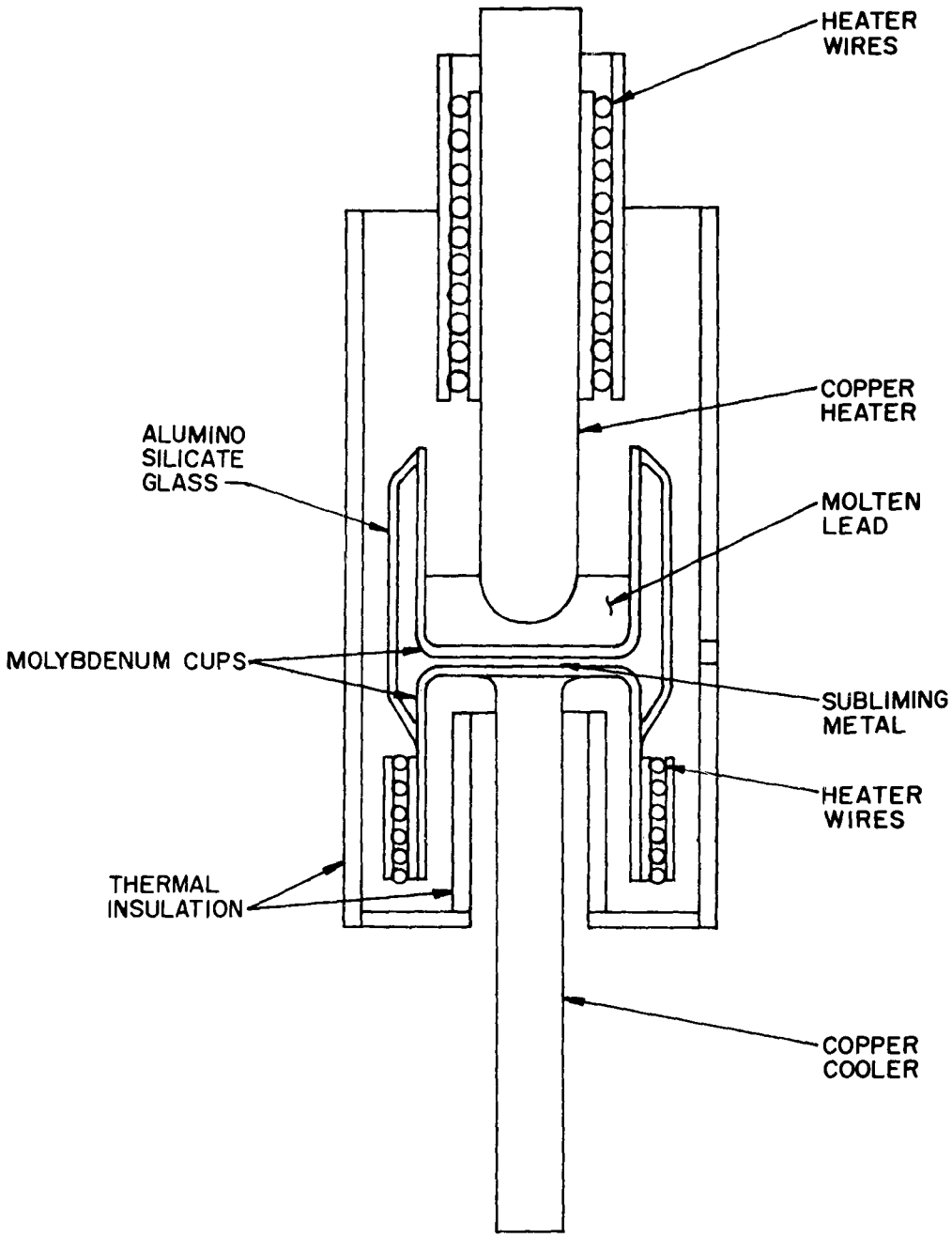

Fig. 19 - Transparent Test Cell for Observations on Subliming Cadmium

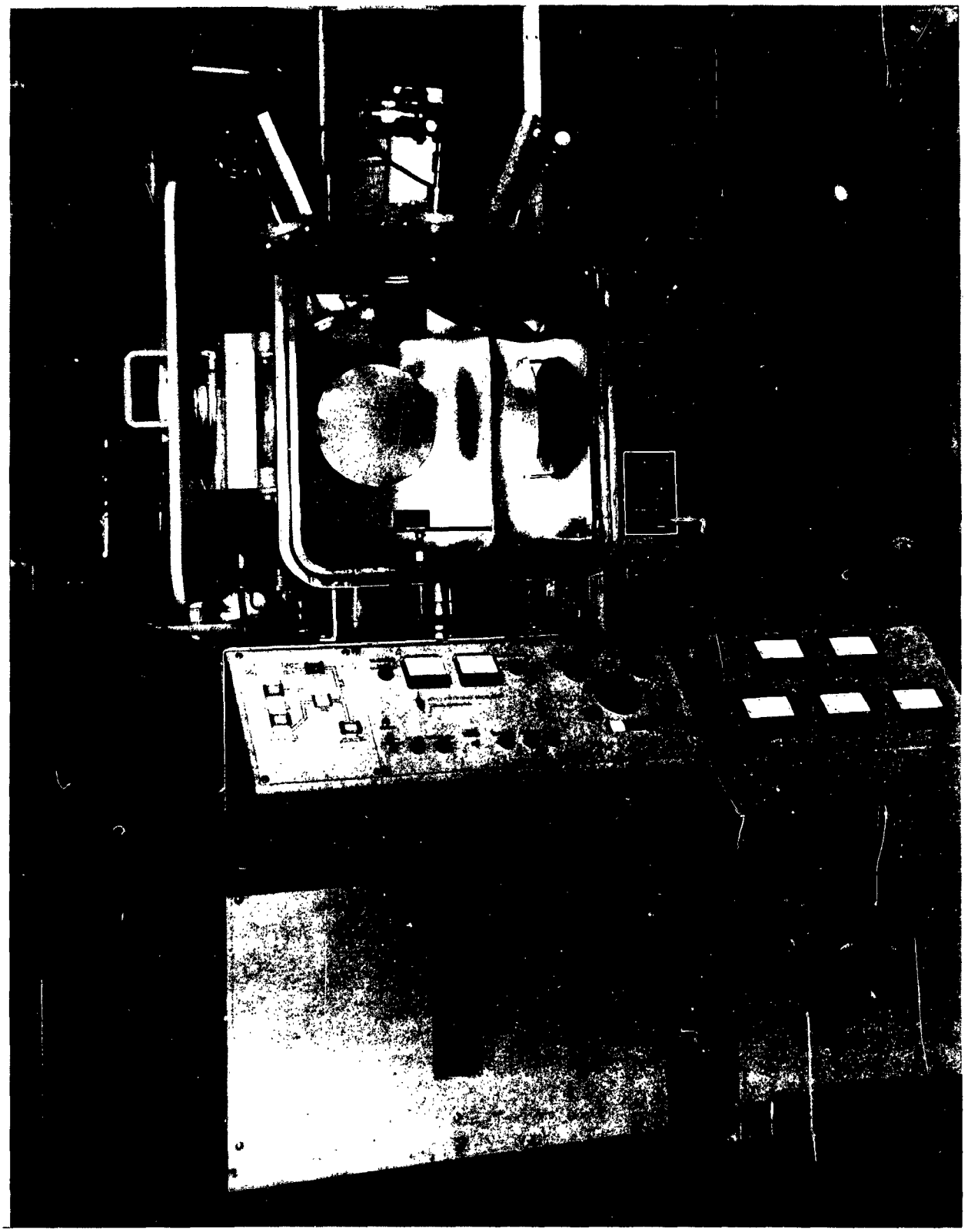

Fig. 20 - High Voltage Electron Beam Equipment

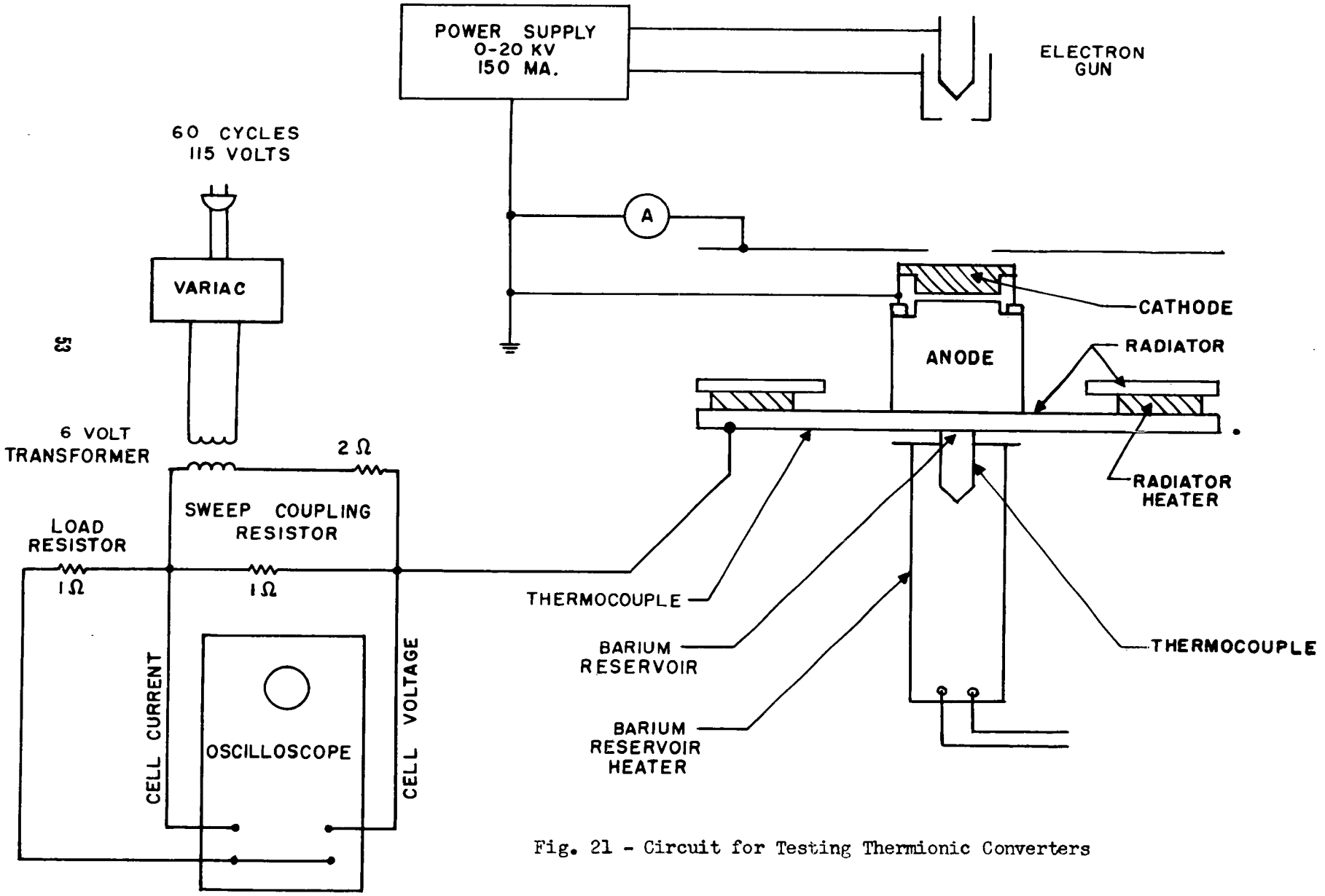

Fig. 21 - Circuit for Testing Thermionic Converters

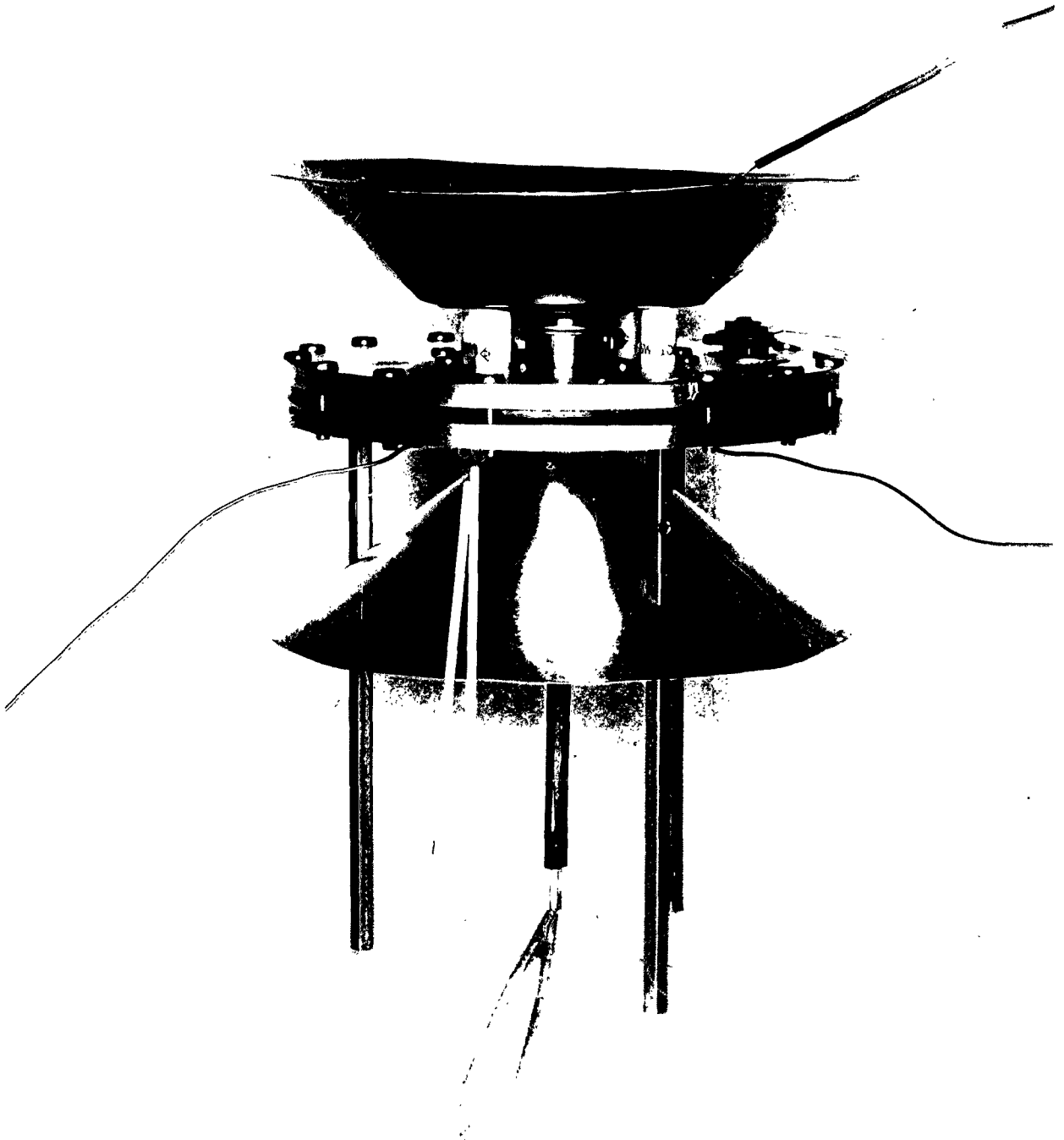

Fig. 22 - Side View of Thermionic Cell with Radiator, Showing Electron and Thermal Shields

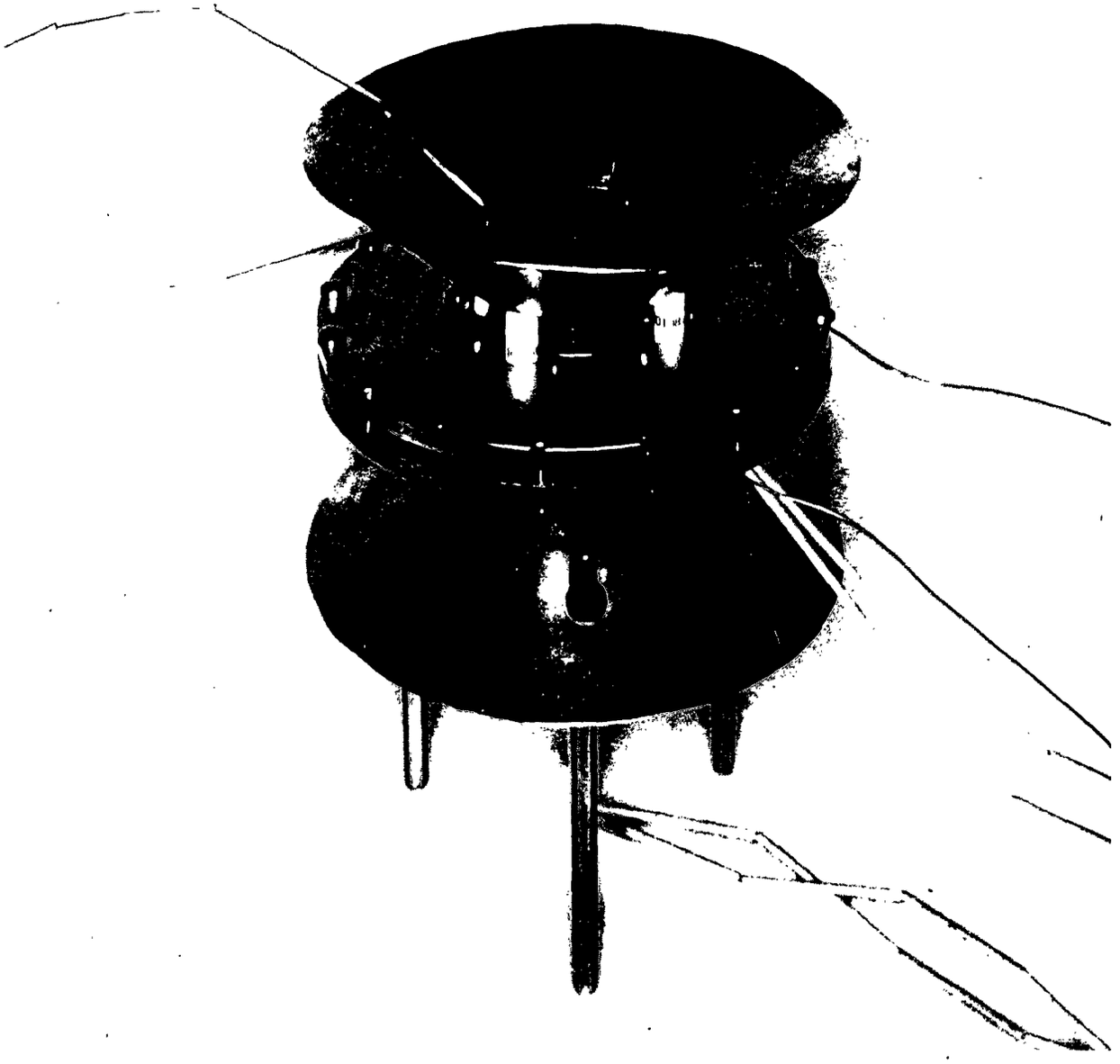

Fig. 23 - Top View of Thermionic Cell with 6" Diameter Radiator and Shields

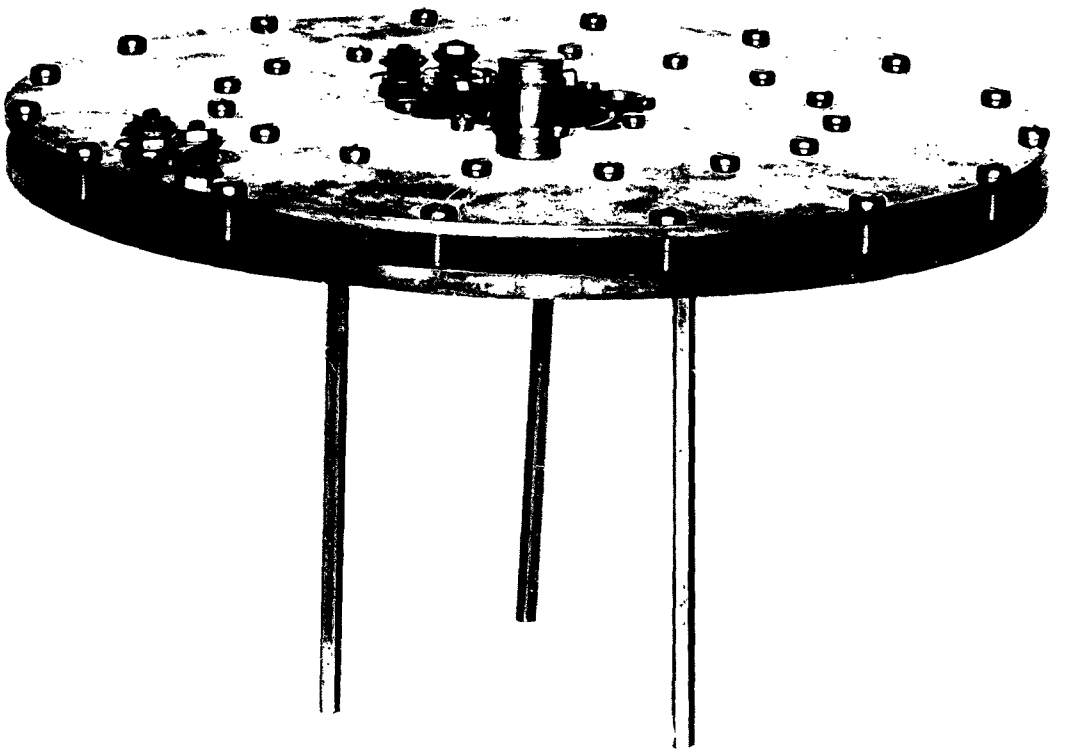

Fig. 24 - Thermionic Cell with 12" Diameter Radiator

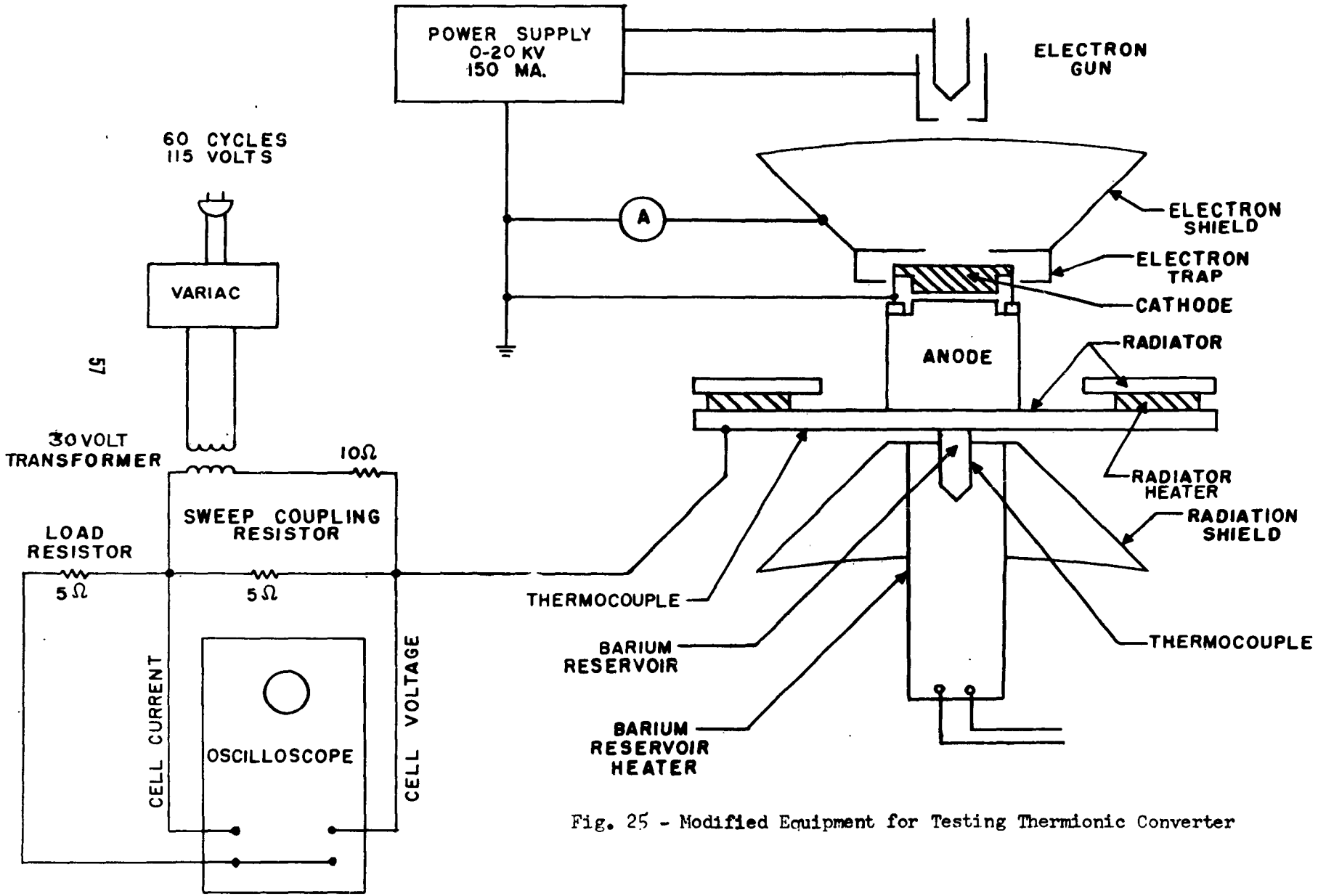

Fig. 25 - Modified Equipment for Testing Thermionic Converter

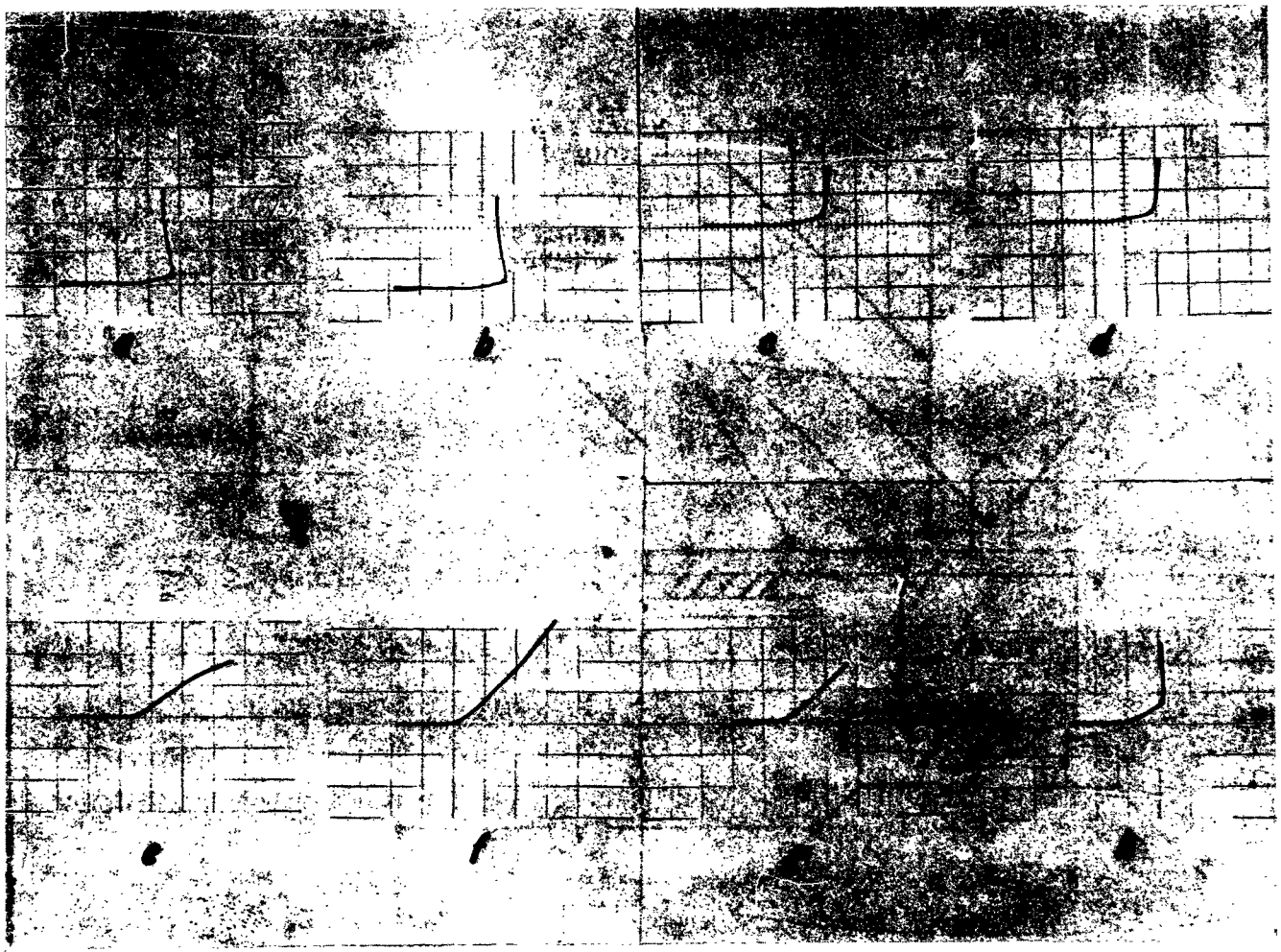

Fig. 26 - Experimental Current-Voltage Curves

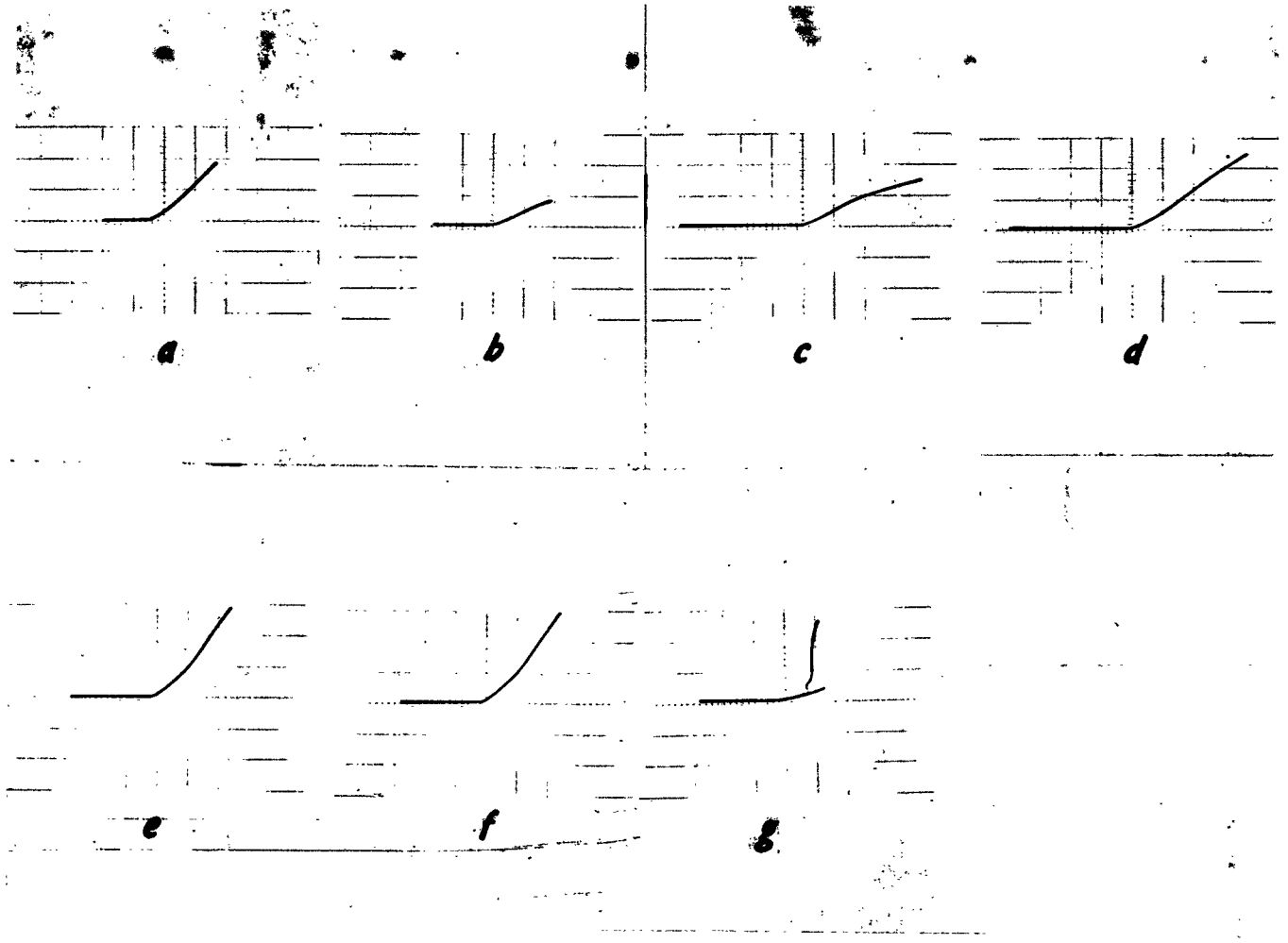

Fig. 27 - Experimental Current-Voltage Curves

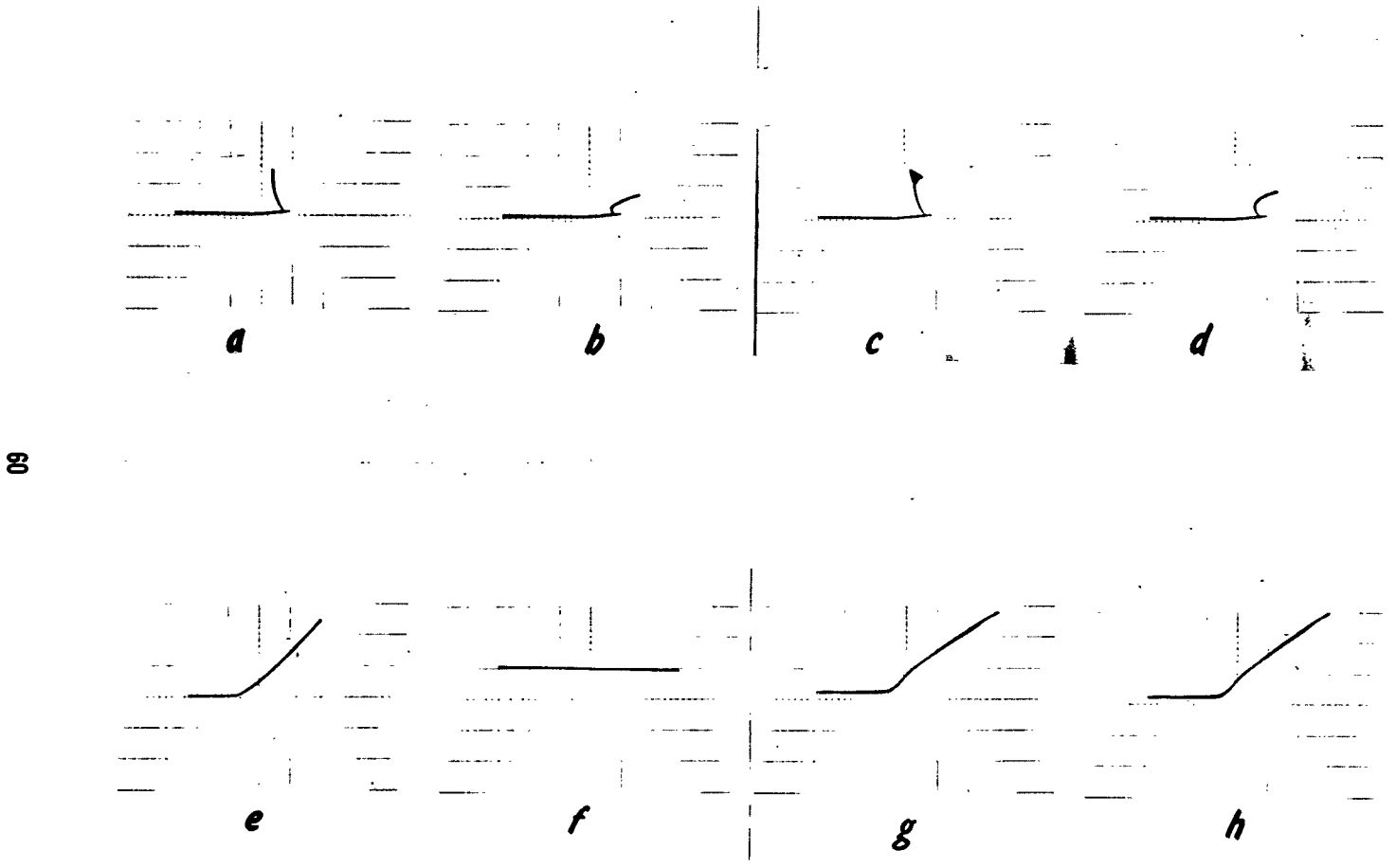

Fig. 28 - Experimental Current-Voltage Curves

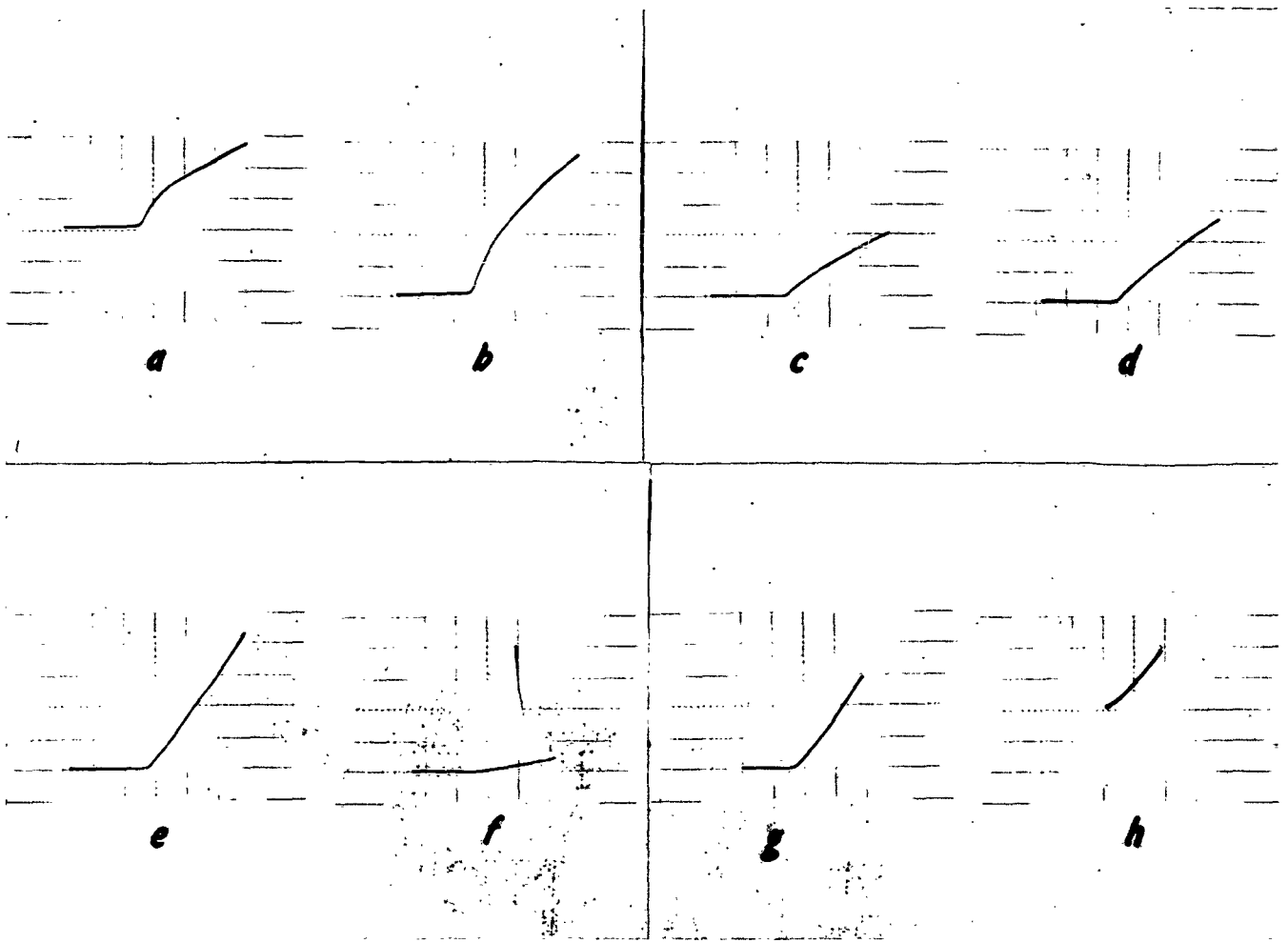

Fig. 29 - Experimental Current-Voltage Curves

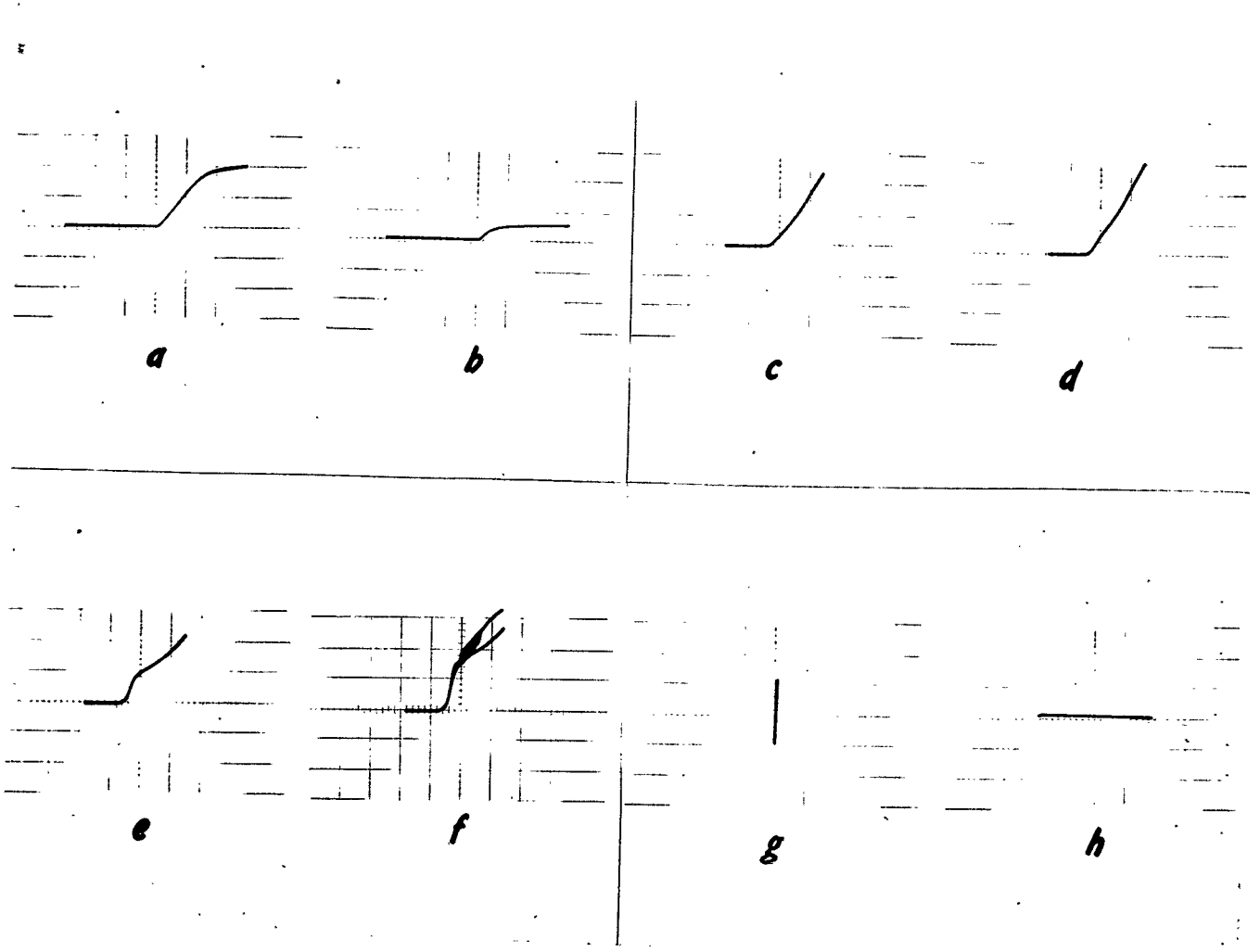

Fig. 30 - Experimental Current-Voltage Curves

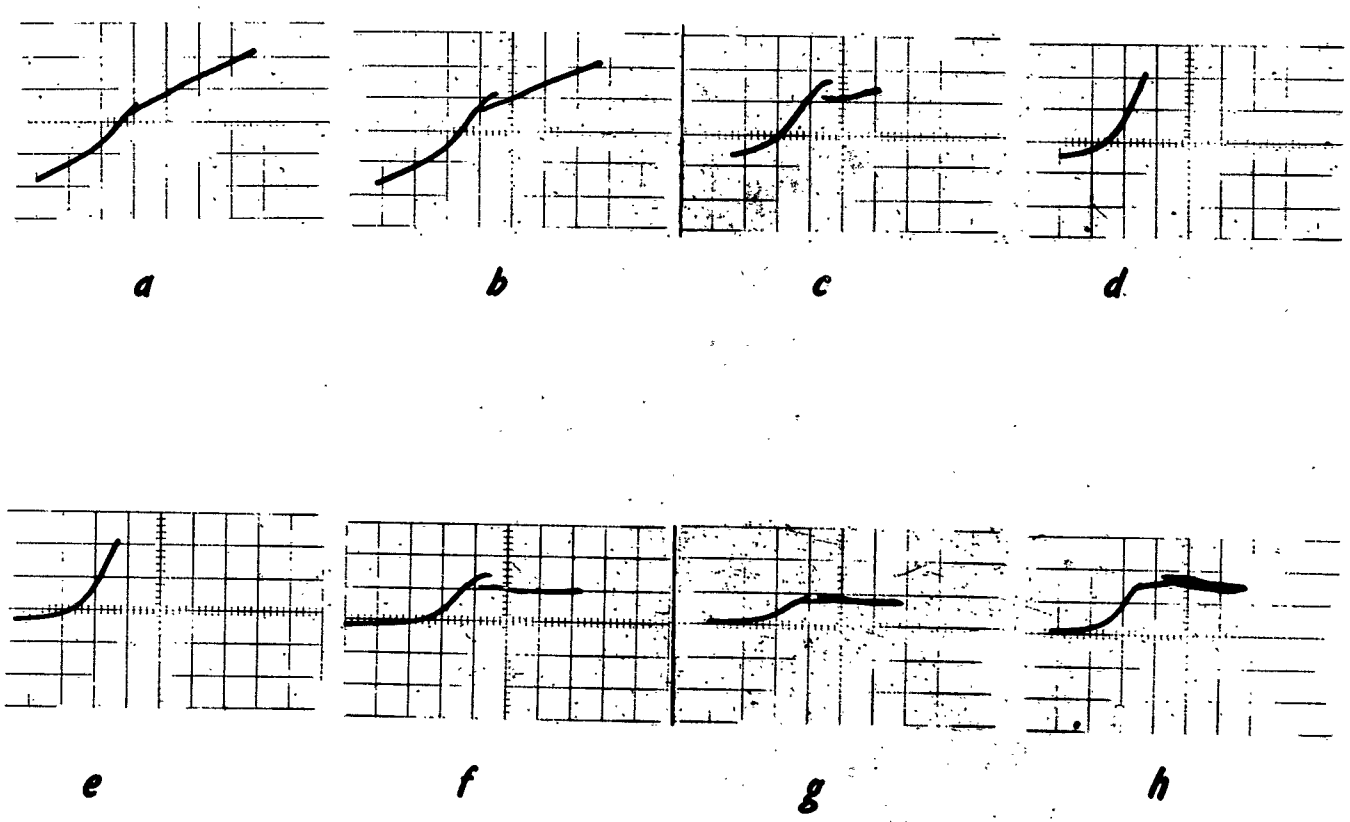

Fig. 31 - Experimental Current-Voltage Curves

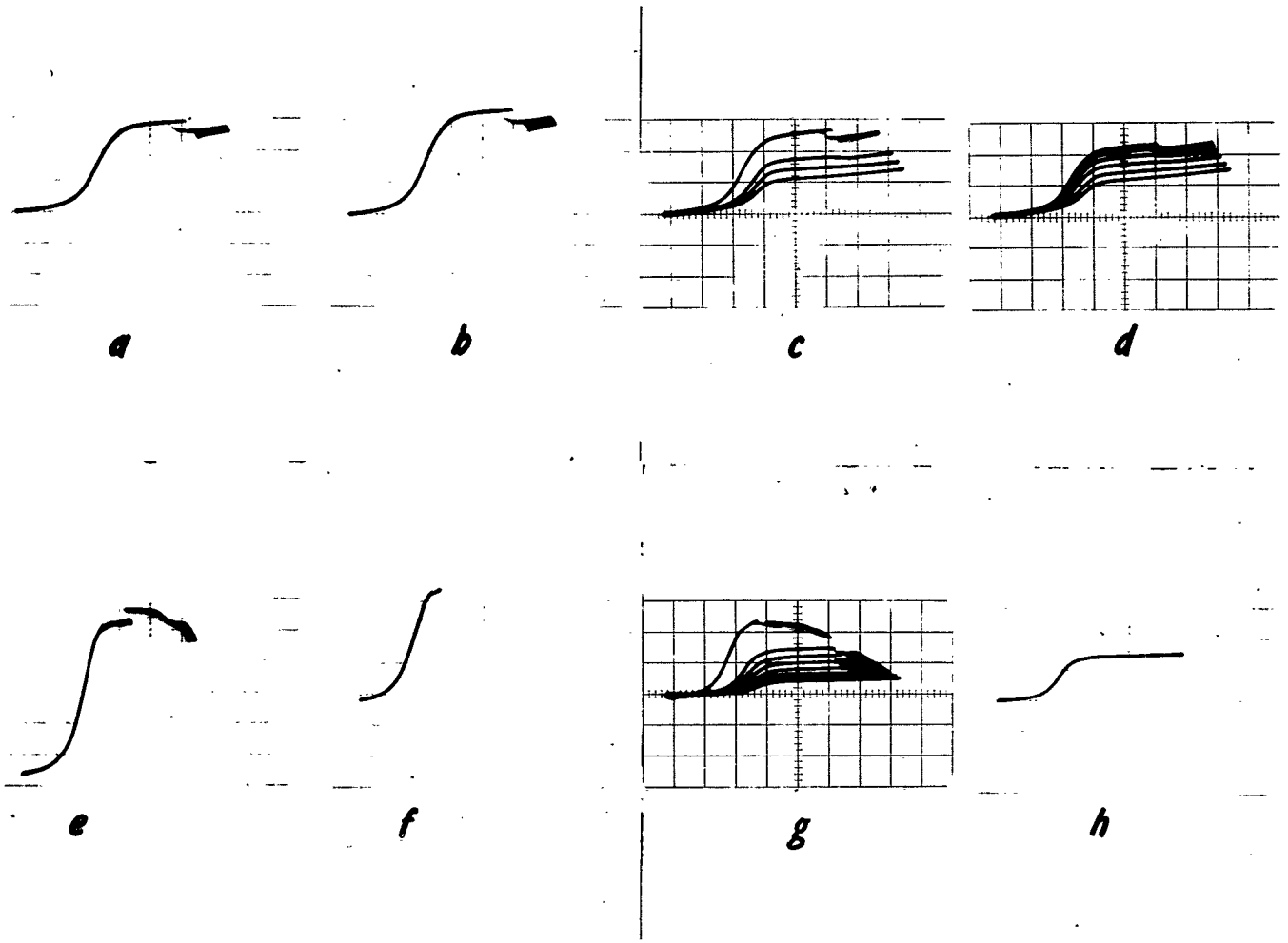

Fig. 32 - Experimental Current-Voltage Curves

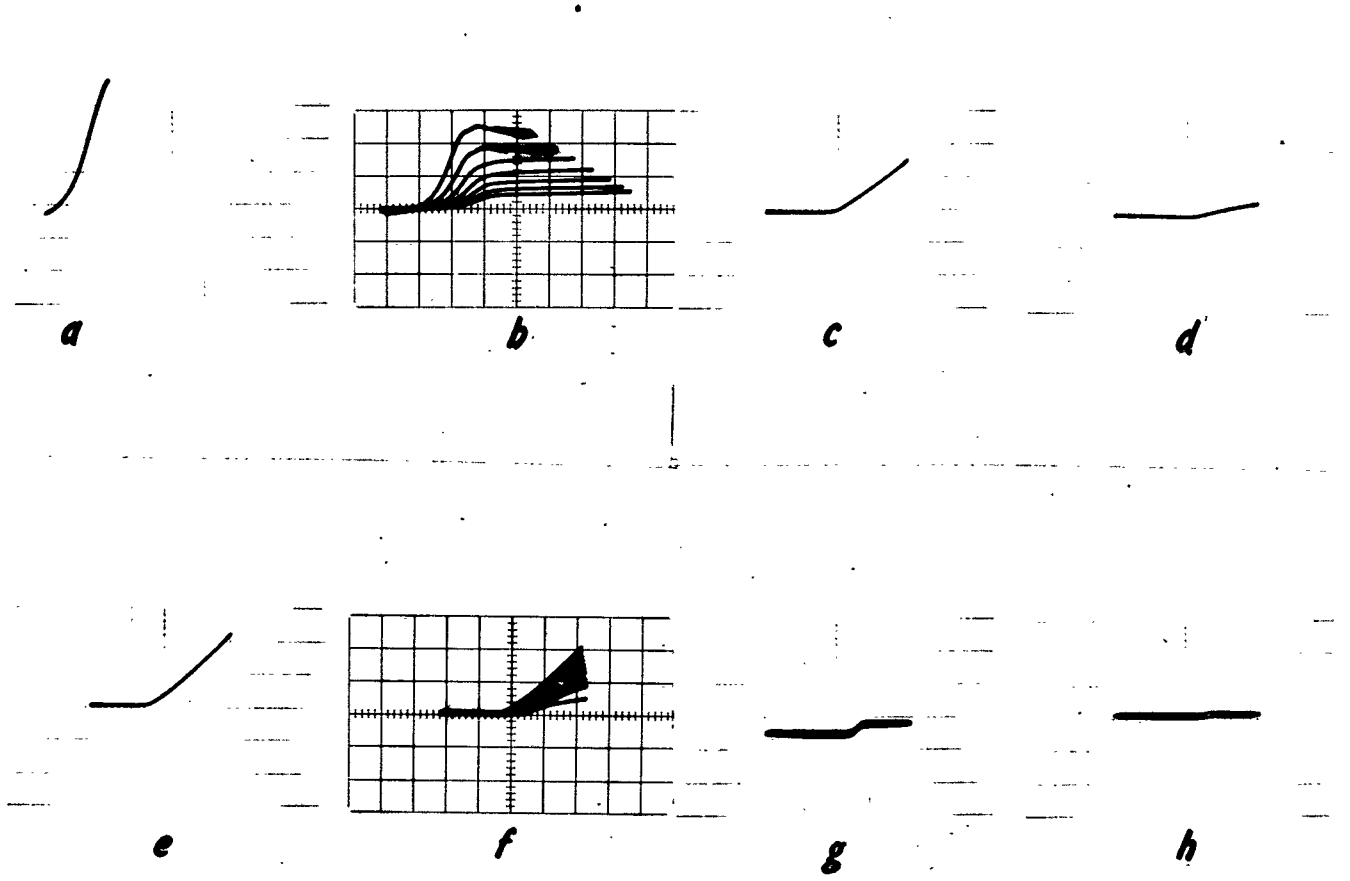

Fig. 33 - Experimental Current-Voltage Curves

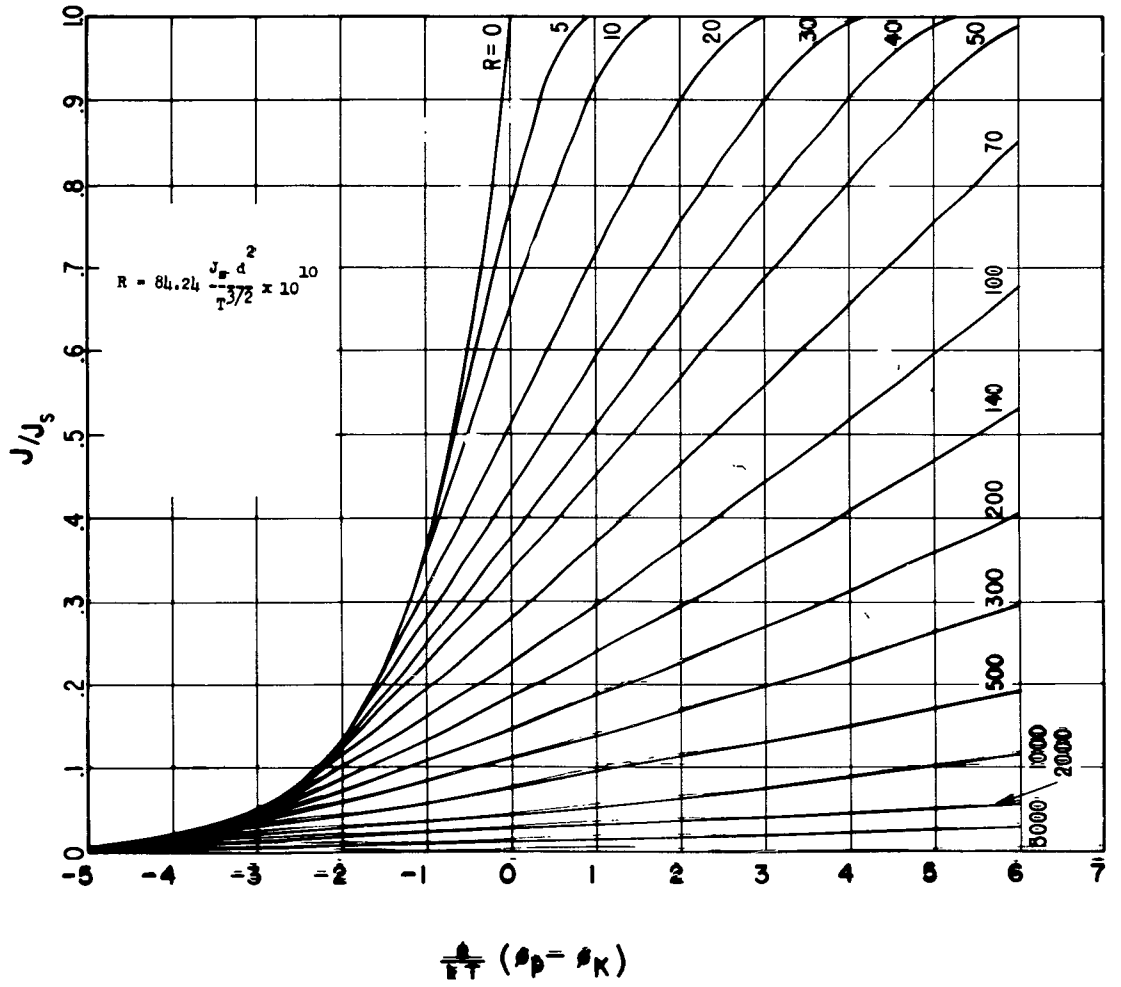

Fig.34 Theoretical Current-Voltage Curves for Vacuum Thermionic Converter
(From W.F.Webster, J.A.P. 30, 490, 1959)

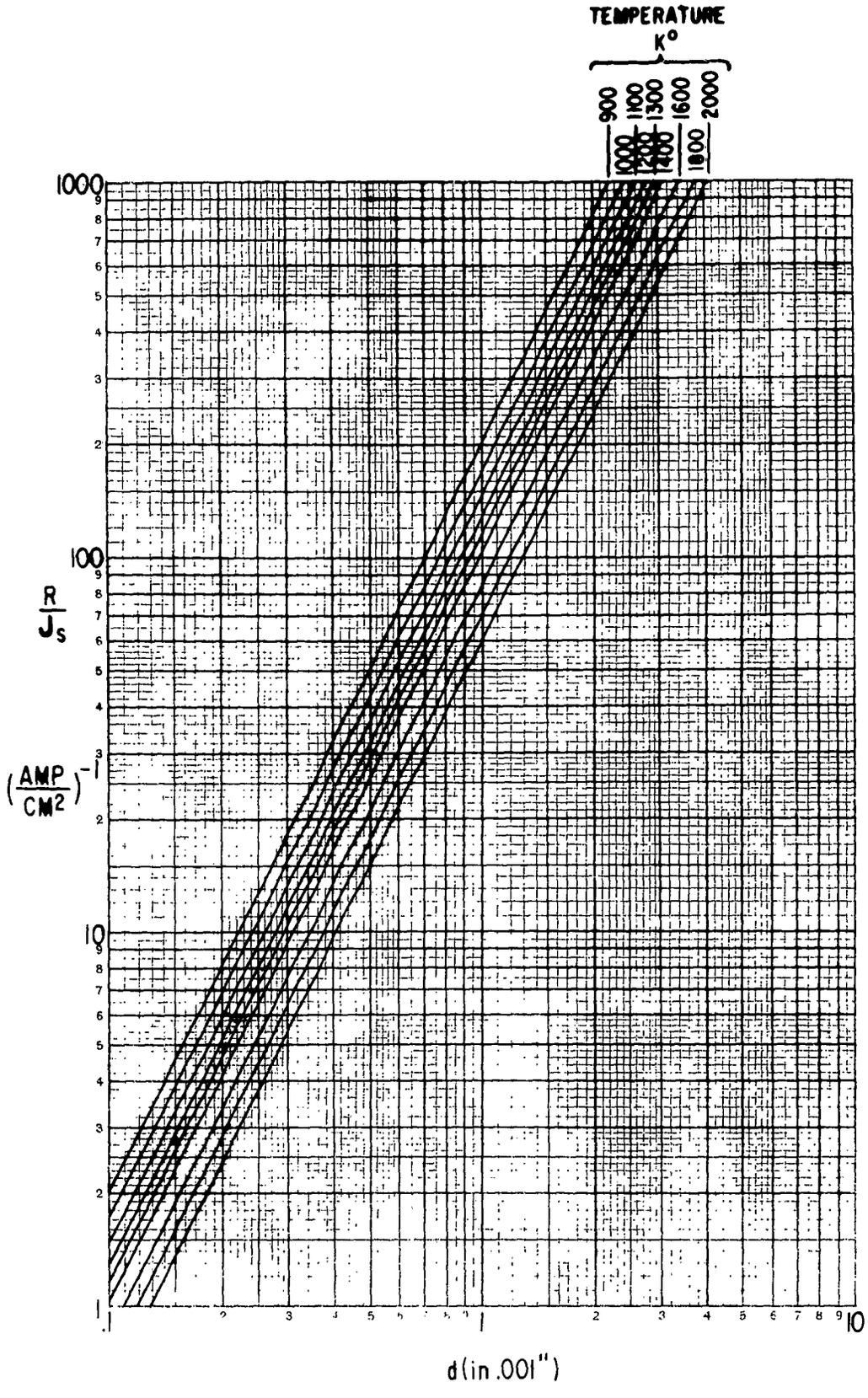

Fig. 35 - R/J_s vs d for Nine Cathode Temperatures (From H. F. Webster, J.A.P. 30, 490, 1959)

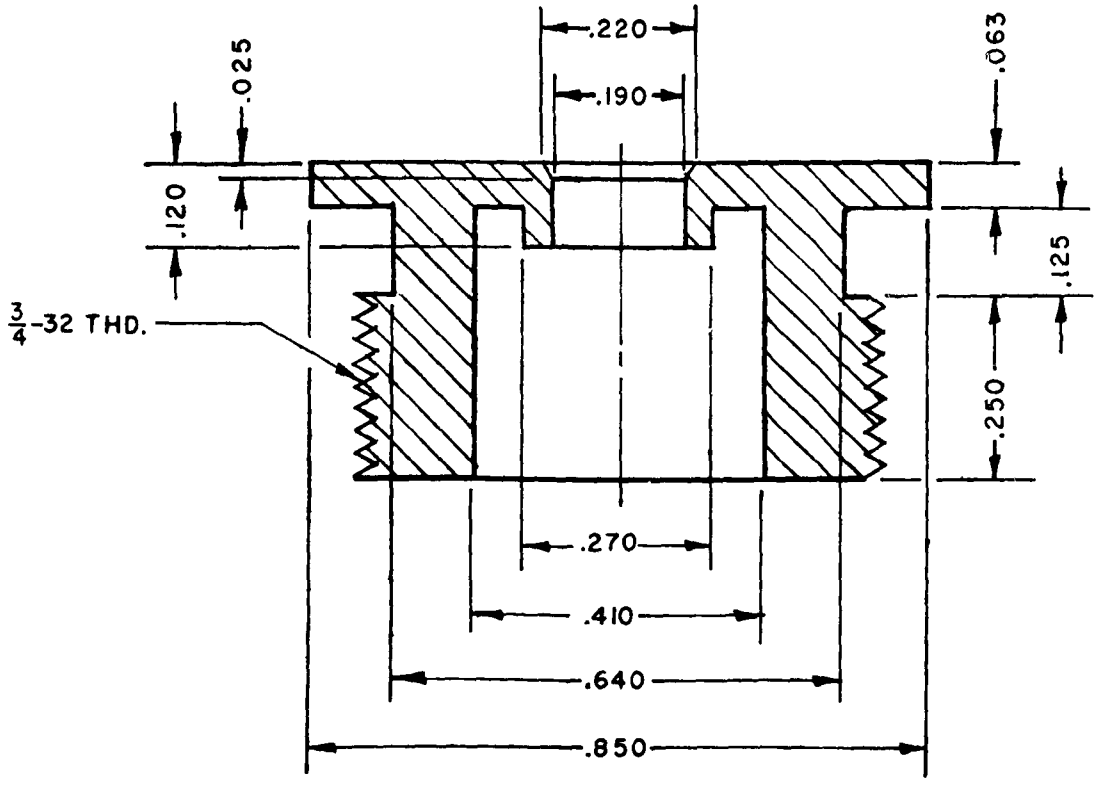

Fig. 36 - Anode Design for Improved Localization of Barium Deposit

BIBLIOGRAPHY

1. Huston, J. M., Theoretical Efficiency of the Thermionic Energy Converter, Journal of Applied Physics 30, 481-7 (1959).

2. Dushman, Saul. Vacuum Technique, Wiley and Sons, Inc., p. 746, 1949.

3. Webster, H. F., Calculation of the Performance of a High Vacuum Thermionic Energy Converter, Journal of Applied Physics 30, 488-92 (1959).

4. Ashworth, F., Advances in Electronics III, Academic Press, Edited by L. Marton, pp 17, 18.

5. Coomes, E. A., Electron Emission from a Single Crystal, ASTIA Reprint No. 229, 451 (Unclassified).

6. Rasor, N. S., Figure of Merit for Thermionic Energy Conversion, Journal of Applied Physics 31, 163-7 (1960).

7. Rittner, E. S., On the Theory of the Close-Spaced Impregnated Cathode Thermionic Converter, Journal of Applied Physics 31, 1065-71 (1960).

8. Kaye, J. and Welsh, J. A., Direct Conversion of Heat to Electricity, Wiley and Sons, Inc., 1960.

9. Nottingham, W. B., Thermionic Energy Converter, MIT Technical Report 373, Sept. 9, 1960.

10. Epstein, P. S., Textbook of Thermodynamics, Wiley and Sons, Inc., p. 157, 1937.

11. Becker, J. A., The Use of the Field Emission Microscope in Adsorption Studies of Ba on W, Bell System Technical Journal 30, 907-932 (1951).

12. Kohl, W. H., Materials and Techniques for Electron Tubes, Reinhold Publishing Co., 1960. p. 535.

APPENDIX A

SUMMARY OF TEST RESULTS

Tests were carried out in a vacuum chamber with the cathode heated by a high voltage electron beam. The anode was cooled by a radiator, which could also be electrically heated. The barium reservoir had a separate electrical heater, but the effective reservoir temperature was found to depend somewhat on the anode and cathode temperatures.

Starting with an anode-cathode spacing of 0.007 inch, currents of several milliamperes were observed at first. These currents tended to be limited by space charge at low voltages and by saturated emission at high voltages. When barium was sublimed into the anode-cathode space, by heating the barium reservoir, a large increase in cathode emission was observed, due to a thin film of barium atoms on the cathode surface. At the lower barium pressures and higher cathode temperatures, the film of barium atoms was less than a monolayer thick; for cooling of the cathode invariably produced an immediate increase of cathode emission. This was due to a reduction of cathode work function which more than offset the reduction in cathode temperature. As the cathode temperature dropped further, the cathode emission reached a maximum and then decreased. This peak of the Taylor-Langmium S-curve was repeatedly traversed.

As the temperature of the barium reservoir was raised, barium began to condense on the anode surface and reduce the anode-cathode spacing. By thus reducing the spacing, greatly increased currents were recorded. Metallic contacts between anode and cathode were observed several times, but these could be eliminated by heating the cathode above 1000 degrees C and heating the anode to its proper operating temperature of 500 degrees C.

The highest power output recorded was 0.28 ampere per square centimeter at a back bias of 0.7 volt. This is not considered a measure of maximum power, for optimum conditions could not be explored systematically. The top part of the barium reservoir was inaccessible for proper heating, and reservoir heaters were repeatedly burned out attempting to drive barium out of this part of the reservoir. This defect can be remedied by a modification of the anode design, but time did not permit this modification.

APPENDIX B

TRANSIENT SOLUTION FOR INTERNAL SURFACE TEMPERATURE OF THERMIONIC CONVERTER ANODE

A number of simplifying assumptions have been made to determine analytically the transient response of the internal surface temperature of the anode of the thermionic diode.

1. The mathematical model is assumed to be a plate of infinite extent with thickness b.

2. The thermal properties of the material are assumed to be constant with respect to temperature.

3. The boundary conditions are assumed to be:

   a. Temperature maintained at zero at x = 0 (the external surface of the anode);

   b. A constant heat flux of Q is maintained at x = b (the internal surface of the anode).

4. The initial condition is assumed to be: anode at temperature equal to zero.

The transient solution for this set of conditions is detailed in "Condition of Heat in Solids" by Carslaw and Jaeger, p. 104, Section 43ii:

$$v = \frac{Qx}{K} - \frac{8Qb}{K\pi^2} \sum_{n=0}^{\infty} \frac{(-1)^n}{(2n+1)^2} e^{-\frac{K(2n+1)^2\pi^2}{cp\,4b^2}t} \sin\frac{(2n+1)\pi x}{2b} \qquad \text{(B-1)}$$

where

v = temperature
Q = heat flow
x = distance within anode thickness
K = thermal conductivity
b = anode thickness
c = specific heat
p = mass density
t = time

Of major interest is the transient temperature response of the inner surface of the anode (x = b). Equation (B-1) then simplifies to:

$$v = \frac{Qb}{K}\left[1 - \frac{8}{\pi^2}\sum_{n=0}^{\infty}\frac{1}{(2n+1)^2}\, e^{-\frac{K(2n+1)^2\pi^2}{cp\ 4b^2}t}\right] \qquad \text{(B-2)}$$

The variables in Equation (B-2) may be grouped as follows for the generalized dimensionless plot of Figure (B-1).

$$\theta = 1 - \frac{8}{\pi^2}\sum_{n=0}^{\infty}\frac{1}{2n+1}\, e^{-\frac{\pi^2}{4}(2n+1)^2\beta} \qquad \text{(B-3)}$$

where

$$\theta = \frac{vK}{Qb} \qquad \beta = \frac{K}{cp}\ \frac{t}{b^2}$$

Equation (B-3) may be evaluated for the following physical parameters that are representative of the experimental diode model at 500 degrees C:

b = 0.3 cm
K = 0.226 watts/cm ^{o}C
cp = 4.82 joules/cm^3 ^{o}C
Q = watts/cm^2

The time for the surface temperature to rise to 63 percent of its equilibrium value (time constant) for the above conditions is 0.67 seconds.

Fig. B-1 - Temperature Rise of Thermionic Converter Anode Surface as a Function of Time

APPENDIX C

STEADY STATE TEMPERATURE DISTRIBUTION PRODUCED BY A SOURCE OF HEAT ON ONE SURFACE OF A LOW CONDUCTIVITY SLAB WITH A PERFECT THERMAL CONDUCTOR ON THE OTHER SIDE

We are concerned first with the temperature on the top surface of a slab of thickness, b, and of low thermal conductivity, K, due to a point heat source of q watts. The other side of the slab is considered to be held at constant temperature, T_0. Referring to Figure C-1A, cylindrical coordinates r and z are used, and the heat source is located at the origin. By symmetry it is clear that the upper surface temperature will be the same as in Figure C-1B, where the slab has a thickness 2b and a heat sink of the same wattage is placed on the lower side directly opposite the heat source. Laplace's equation is assumed to hold in all three regions. Then the temperature can be expanded in an infinite series of Bessel Functions, which are solutions of Laplace's equation in cylindrical coordinates[1].

$$T^2 = \frac{q}{4\pi K}\left[\int_0^\infty \psi(k)\, J_0(kr)\, e^{-kz}\, dk + \int_0^\infty \Theta(k)\, J_0(kr)\, e^{kz}\, dk\right] \qquad \text{(C-1)}$$

The value of ψ and θ may be found by applying the boundary condition that the normal flow of heat at each point of the external surfaces is zero, and that the total flow of heat across the plane z = b is equal to q. Making use of some general equations of Smythe[1] and expanding in a power series in b/r we find

$$(\Delta T)_p = \frac{4\, b^2\, q}{\pi K\, r^3} \qquad (r/b > 1) \qquad \text{(C-2)}$$

The temperature drop at a distance r due to a point source flowing throughout a sphere is

$$(\Delta T)_s = \frac{q}{4\pi r K} \qquad (r/b > 1) \qquad \text{(C-3)}$$

while the temperature associated with hemispherical flow is

$$(\Delta T)_h = \frac{q}{2\pi r K} \qquad \text{(C-4)}$$

---

1 See W. R. Smythe. Static and Dynamic Electricity, 2nd Ed. New York. McGraw-Hill, 1950 Page 182.

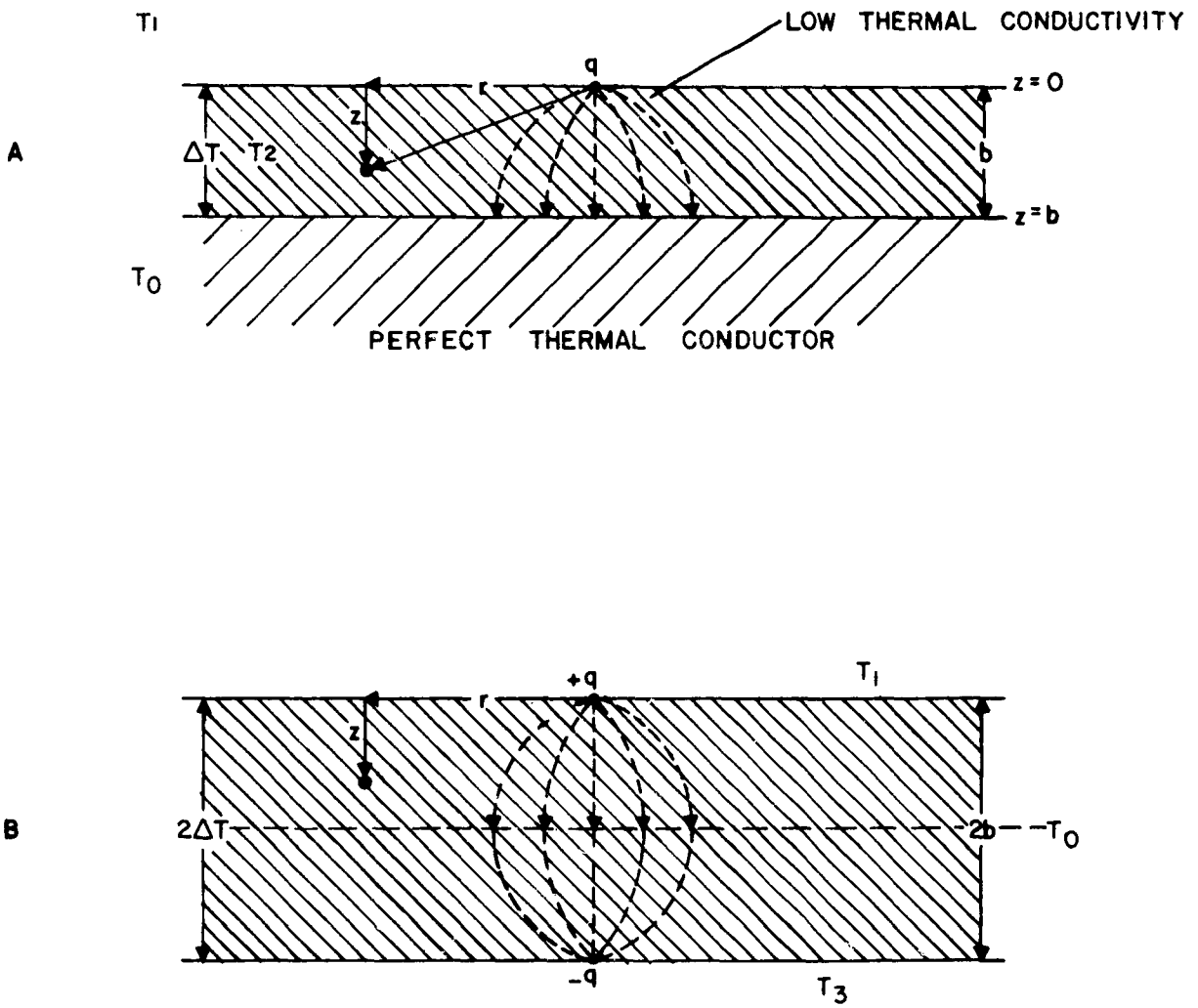

Fig. C-1 - Steady State Temperature Distribution in Anode Decoupling Layer

Thus the relative decrease of temperature differential due to a backing of material of high thermal conductivity, found by dividing equation (C-4) by equation (C-2) is

$$\frac{(\Delta T)_p}{(\Delta T)_h} = \frac{8\,b^2}{r^2} \qquad \text{(C-5)}$$

The temperature drop due to a line source of heat equal to q' watts per cm is found by integrating equation (C-2) along the line

$$\Delta T = \frac{8\,b^2\,q'}{\pi\,a^2 K}$$

where a is the distance to the line.

Thus in the case of a point source of heat, the temperature rise outside of the circle $r = b$ falls off as the inverse cube or r. In the case of an infinite line source of heat, the temperature rise at a distance greater than the slab thickness falls off as the inverse square of the distance.

APPENDIX D

COLLAPSING PRESSURE OF THIN WALLED CYLINDRICAL VESSELS

The currently conceived configuration for the design of the thermionic diode involves a cylindrical capsule having heavy top and bottom walls (anode and cathode) but very thin cylindrical walls to minimize the heat conduction between the anode and cathode. The current laboratory model is being constructed of tantalum tubing having a diameter of 1.5 inches, 0.004-inch wall thickness, and a length of 0.25 inches welded to a heavy tungsten anode and cathode. The capsule is subjected to an external pressure load of essentially a full atmosphere since the interior is evacuated. The collapsing pressure for the configuration may be determined by application of the following formula (Ref: Formulas for Stress and Strain by R. J. Roarke):

$$P = \frac{E\left(\frac{t}{r}\right)}{1 + \frac{1}{2}\left(\frac{\pi r}{nl}\right)^2} \left\{ \frac{1}{n^2\left[1 + \left(\frac{nl}{\pi r}\right)^2\right]^2} + \frac{n^2 t^2}{12\, r^2 (1 - \nu^2)} \left[1 + \left(\frac{\pi r}{nl}\right)^2\right]^2 \right\}$$

where:

P = collapsing pressure
E = elastic modulus - lb/in.^{2}
t = wall thickness - in.
r = tube radius - in.
l = tube length - in.
n = collapsing mode = 2, 3, 4, ---- n
ν = Poisson's ratio

The collapsing mode is not known; the equation must be evaluated by plotting P versus n where n is any positive integer equal to or greater than two. The capsule cylindrical side walls will collapse at a pressure corresponding to the minimum of this curve. For the laboratory model:

r = 0.75 in.
l = 0.25 in.
t = 0.004 in.
E = 27 x 10^6 lb/in.^{2}
ν = 0.35

The collapsing pressure is approximately 285 lb/in.^{2} which provides a factor of safety of approximately 20.

With a change in capsule diameter to 0.75 in. (second laboratory model), the other variables remaining unchanged, the collapsing pressure is in excess of 500 lb/in^2.

Aeronautical Systems Division, Dir/Aeromechanics, Flight Accessories Lab, Wright-Patterson AFB, Ohio.
Rpt Nr ASD-TDR-62-687, INVESTIGATION OF CLOSE-SPACED THERMIONIC CONVERTER. Final report, Oct 62, 77 p. incl. illus., tables, 12 refs.

Unclassified Report

Difficulties in realizing a very small anode cathode spacing, due to uneven thermal expansion and warping, have led to a feasibility study of a subliming anode surface that automatically maintains the proper spacing from the cathode. Barium was chosen as a subliming metal since it serves also to activate the cathode. This required that all parts of the vacuum enclosure be held above 500°C. Effects of barium corrosion at high temperatures were studied. Four test models were made and tested. Starting with an anode-cathode spacing of 0.007 inch and a heated barium reservoir, the spacing was reduced by build-up of barium on the anode. The characteristic thermionic current-voltage curves were seen, with currents twelve times larger than those obtainable with the original spacing. The highest power output observed was 0.28 amperes/cm^2 at 0.7 volt. Since the temperature distribution in the anode was non-optimum, suggestions are made for further studies with improved anode design.

(over)

1. Generators
2. Thermionic Converters
3. Diodes
4. Servo mechanisms

I. AFSC Project 8173, Task 817305
II. AF33(616)-7683
III. ITT Industrial Laboratories, Fort Wayne, Indiana
IV. D. K. Coles
V. Aval fr OTS
VI. In ASTIA collection

Aeronautical Systems Division, Dir/Aeromechanics, Flight Accessories Lab, Wright-Patterson AFB, Ohio.
Rpt Nr ASD-TDR-62-687, INVESTIGATION OF CLOSE-SPACED THERMIONIC CONVERTER. Final report, Oct 62, 77 p. incl. illus., tables, 12 refs.

Unclassified Report

Difficulties in realizing a very small anode cathode spacing, due to uneven thermal expansion and warping, have led to a feasibility study of a subliming anode surface that automatically maintains the proper spacing from the cathode. Barium was chosen as a subliming metal since it serves also to activate the cathode. This required that all parts of the vacuum enclosure be held above 500°C. Effects of barium corrosion at high temperatures were studied. Four test models were made and tested. Starting with an anode-cathode spacing of 0.007 inch and a heated barium reservoir, the spacing was reduced by build-up of barium on the anode. The characteristic thermionic current-voltage curves were seen, with currents twelve times larger than those obtainable with the original spacing. The highest power output observed was 0.28 amperes/cm^2 at 0.7 volt. Since the temperature distribution in the anode was non-optimum, suggestions are made for further studies with improved anode design.

(over)

1. Generators
2. Thermionic Converters
3. Diodes
4. Servo mechanisms

I. AFSC Project 8173, Task 817305
II. AF33(616)-7683
III. ITT Industrial Laboratories, Fort Wayne, Indiana
IV. D. K. Coles
V. Aval fr OTS
VI. In ASTIA collection